Future trend and sensitivity analysis of evapotranspiration in the Senegal River Basin

Papa Malick Ndiaye, Ansoumana Bodian, Lamine Diop, Alain Dezetter, Etienne Guilpart, Abdoulaye Deme, Andrew Ogilvie

Journal of Hydrology: Regional Studies 35 (2021) 100820

Contents lists available at ScienceDirect

Journal of Hydrology: Regional Studies

journal homepage: www.elsevier.com/locate/ejrh

Future trend and sensitivity analysis of evapotranspiration in the Senegal River Basin

Papa Malick Ndiaye [a], Ansoumana Bodian [a,*], Lamine Diop [b], Alain Dezetter [c], Etienne Guilpart [d], Abdoulaye Deme [e], Andrew Ogilvie [f]

[a] Laboratoire Leïdi "Dynamique des Territoires et Développement", Université Gaston Berger (UGB), Saint Louis, Senegal
[b] UFR S2ATA Sciences Agronomiques, de l'Aquaculture et des Technologies Alimentaires, Université Gaston Berger, Saint-Louis, Senegal
[c] HydroSciences Montpellier, Univ Montpellier, IRD, CNRS, CC 057, 163 rue Auguste Broussonnet, 34090, Montpellier, France
[d] Département de génie civil et de génie des eaux, Université Laval, 2325 Rue de l'Université, Québec, QC, G1V 0A6, Canada
[e] Laboratoire LSAO "Laboratoire des Sciences de l'Atmosphère et de l'Océan", Université Gaston Berger (UGB), BP 234, Saint-Louis, Senegal
[f] UMR G-EAU, AgroParisTech, Cirad, Institut Agro, INRAE, IRD, Univ Montpellier, 34196, Montpellier, France

ARTICLE INFO

Keywords:
Evapotranspiration
Climate change
Trend
Sensitivity coefficient
Climate models
Senegal River basin

ABSTRACT

Study region: Senegal River Basin in West Africa.
Study focus: This work aimed to assess reference evapotranspiration (ET_0) trends and its sensitivity to climate variables on the period 2036–2065 in the Senegal River basin. Seven General Circulation Models (GCMs) and seven Regional Climate Models (RCMs) of the CMIP5 project were used under the scenarios RCP4.5 and RCP8.5. The performance of GCMs and RCMs was first evaluated by comparing their outputs with the reanalyses data. The change of ET_0 is determined between the periods 1971–2000 and 2036–2065. A sensitivity coefficient was calculated to analyze the influence of climatic variables on ET_0. Finally, the Mann Kendall test and Sen slope were used to detect future trends in ET_0 and climate variables.
New hydrological insights for the region: It was found that RCMs were here more robust than GCMs in estimating reference evapotranspiration over the period 1984–2000. Compared to the period 1971–2000, the RCMs show that ET_0 will increase by 14–293 mm under RCP4.5 and by 55–387 mm under RCP8.5 according to the climatic zones. The maximum values are observed in Sahelian zone and the minimum one in Guinean area. The sensitivity analysis shows that ET_0 is more sensitive to relative humidity, maximum temperature and solar radiation. The trend analysis reveals, generally, a significant increase in ET_0 and in maximum and minimum temperatures in the period 2036–2065 under the RCP4.5 and RCP8.5 scenarios. This means that ET_0 will not be stationary and may continue to increase after 2065 because of the increase of temperature.

1. Introduction

Climate change are now affecting both natural and anthropic ecosystems, and are of major concern to the scientific community and policy makers (IPCC, 2018; Ouhamdouch et al., 2020; Bahir et al., 2020). According to the latest estimations from the

* Corresponding author.
E-mail addresses: ndiaye.papa-malick@ugb.edu.sn (P.M. Ndiaye), bodianansoumana@gmail.com, ansoumana.bodian@ugb.edu.sn (A. Bodian), lamine.diop@ugb.edu.sn (L. Diop), Alain.Dezetter@ird.fr (A. Dezetter), etienne.guilpart@gmail.com (E. Guilpart), abdoulaye.deme@ugb.edu.sn (A. Deme), andrew.ogilvie@ird.fr (A. Ogilvie).

https://doi.org/10.1016/j.ejrh.2021.100820
Received 30 November 2020; Received in revised form 24 March 2021; Accepted 5 April 2021
Available online 16 April 2021

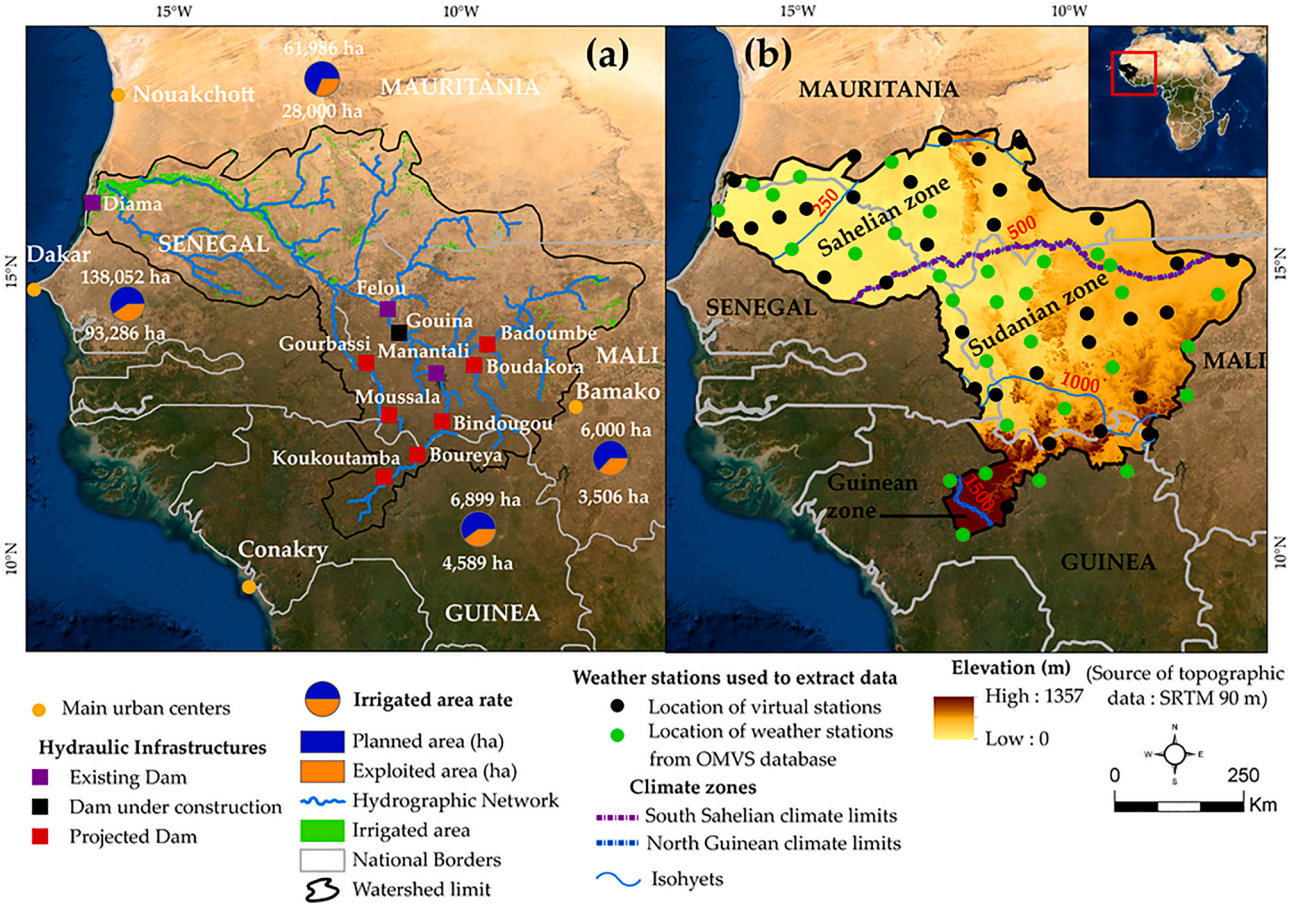

Fig. 1. Senegal river basin: (a) main urban centers, hydraulic infrastructures, irrigated areas by country, (b) stations used to extract data, their altitude and the limits of climatic zones (Ndiaye et al., 2020b).

Intergovernmental Panel on Climate Change (IPCC, 2018), human activities have caused global warming of 1 °C above pre-industrial levels, with a range of 0.8–1.2 °C. This warming could reach 1.5 °C between 2030 and 2052 if it continues to increase at the current rate (IPCC, 2018). This climate change could impact a large panel of sector and activities, by raising pressure on water resources, reducing agricultural productivity, and greater development of vector-borne and water-borne diseases (IPCC, 2014). In addition, a continuous increase in temperatures could intensify the hydrological cycle and lead to the more frequent occurrence of extreme weather events (Chaouche et al., 2010; Tao et al., 2015; Rahman et al., 2018; Wilcox et al., 2018; Ouhamdouch et al., 2020). Therefore, it is important to determine the potential impacts of climate change on water resources and the spatiotemporal variation of hydrological processes.

Reference evapotranspiration (ET_0), a key indicator of climate change, is one of those hydrological processes that directly links the energy balance to the water balance. Evapotranspiration rates mainly depend on the water and energy available and the vapor pressure (Dong et al., 2019). However, these three factors are strongly affected by climate change (Sarkar and Sarkar, 2018). Detecting future changes in evapotranspiration can help to determine the impact of climate change on water resources and to constitute a benchmark for the management of water resources and the optimization of agricultural water demands (Lin et al., 2018; Dong et al., 2019; Mubialiwo et al., 2020). Furthermore, analysis of trends in climatic variables (temperature, wind speed, relative humidity and solar radiation) provides a better understanding of the sensitivity of ET_0 to climate variables and helps determine the potential impacts of climate changes on evapotranspiration (Lin et al., 2018).

In recent years, several authors (Moratiel et al., 2011; Huo et al., 2013; Delghandi et al., 2017; Giménez and García-Galiano, 2018; Dong et al., 2019; Yang et al., 2020; Ouhamdouch et al., 2020) used General Circulation Models (GCMs) or Regional Climatic Models (RCMs) to assess the potential impacts of climate change on evapotranspiration. For example, Dong et al. (2019) used four GCMs to analyze current and future trend of evapotranspiration in an arid and sub-humid climate of Xinjiang province in China according to the RCP4.5 and RCP8.5 scenarios. They concluded that evapotranspiration will continue to increase during the 21 st century. Delghandi et al. (2017) assessed the impacts of climate change on the spatiotemporal variation of ET_0 in an arid and semi-arid climate of Iran using fifteen GCMs. Their results show an increase in evapotranspiration during the periods 2015–2045 and 2070–2099 compared to the period 1971–2000. In the semi-arid zone of Spain, Giménez and García-Galiano (2018) used the average of sixteen regional models to estimate evapotranspiration by the method of Hargreaves and Samani (1985) by 2035 (2021–2050). They noted that ET_0 will continue to rise due to rising temperatures. In West Africa, Obada et al. (2017) used three regional models from the COordinated Regional-climate Downscaling Experiment (CORDEX) project to estimate the annual evapotranspiration in Benin over the period 1951−2100. Their results show an increase in evapotranspiration by 2100 according to the RCP4.5 and RCP8.5 scenarios. To our knowledge, the study of Obada et al. (2017) is the only one that looks at future trends and rate of change in evapotranspiration in West Africa. However, this study did not take into account the sensitivity analysis of ET_0 to climate variables which is an effective way to understand the impact of climate change on evapotranspiration (Wang et al., 2019), and climate projections are not homogeneous across West Africa.

The objective of this work is to analyze the trends of evapotranspiration as well as its sensitivity to climatic variables in the Senegal River basin on the period 2036–2065. Specifically, it seeks to: (i) evaluate the performance of climate models (GCMs and RCMs) compared to reference data for estimating evapotranspiration, (ii) detect future trends in evapotranspiration and climatic variables (temperature, wind speed, relative humidity, radiation solar), (iii) analyze the sensitivity of ET_0 to climatic variables and determine the change rate of ET_0 between the periods 1971–2000 and 2036–2065. Understanding future trends in evapotranspiration is essential to assess the impact of climate change on water resources and develop adequate and efficient management strategies, notably in the Senegal River Basin where resources are under increasing pressure to supply agriculture, hydroelectric production, drinking water, navigation, etc.

2. Materials and methods

2.1. Study area

The Senegal River basin is the second largest transboundary basin in West Africa. It covers an area over of 300,000 km^2 and its population is estimated at 6.5 million in 2015 and could reach 9.5 million in 2025 (SDAGE-OMVS, 2009). The basin spans four states (Guinea, Mali, Mauritania, Senegal) which created the Organization for the Development of the Senegal River (in french, l'Organisation pour la Mise en Valeur du fleuve Sénégal, OMVS). The Senegal River basin is at the heart of the socio-economic development strategies of the riparian countries. The establishment of hydraulic infrastructure (Fig. 1a) has enabled agricultural development, hydroelectric production and the exploitation of mineral resources. From a climatic point of view, the longitudinal distribution of precipitation divides the basin into three climatic zones: Sahelian, Sudanian and Guinean (Dione, 1996; Fig. 1b). The Sahelian zone occupies 37 % of the basin and the average annual rainfall is less than 500 mm over the period 1951−2004. In the Sudanian zone (62 % of the basin area), the annual average precipitation varies between 500 and 1500 mm. The Guinean zone (1%) records the most abundant precipitations with an average greater than 1500 mm. The daily maximum temperature can reach 43 °C in Guinean area, 48 °C in the Sahelian zone and 49 °C in Sudanian area over the period 1984–2017. The Sahelian zone is here influenced by the sea leading to a dampening of temperatures.

2.2. Data

In this study, data from reanalysis, General Circulation Models (GCMs) and Regional Climate Models (RCMs) are used.

Reanalysis weather data from the NASA Langley Research Center (LaRC) POWER project driven by NASA Earth Science/Applied

Science program (https://power.larc.nasa.gov/data-accessviewer, accessed December 20, 2018) are used as alternatives to observed data generally sparse and inaccessible in Africa (Poccard-Leclercq, 2000; Bodian et al., 2020; Ndiaye et al., 2020a, b). Indeed, too few stations with long time series are available, which represents a major obstacle both to use data from these meteorological stations, but also to carry out an evaluation of any data sets of reanalyses. Thus, NASA reanalyses are used as reference data to assess the spatiotemporal consistency of the outputs of climate models.

In this study, we take into account seven GCMs included in the Coupled Model Intercomparison Project (CMIP5). The seven RCMs datasets used were extracted from the CORDEX-Africa project and the r1i1p1 set, and correspond to the Rossby Center regional atmospheric model (RCA4) which has been forced by the seven GCMs mentioned above (Table 1). The simulation domain spans Longitude: 24 °W-60 °E and Latitude: 45 °S-42 °N. The characteristics of the models used are summarized in Table 1.

The scenarios used are RCP4.5 and RCP8.5. The RCP4.5 scenario recommends stabilizing the concentration of CO_2 with an increase in temperatures of 2.4 °C by 2100 (IPCC, 2014). RCP8.5 is the pessimistic scenario which predicts a high concentration of CO_2 and an increase in temperatures of over 4 °C by 2100 (IPCC, 2014). The multi-model ensemble represents a variety of best effort attempts to simulate the climate system and can provide a consensus representation of the climate system (Taylor et al., 2012; Yin et al., 2015; Dong et al., 2019). In this study, the multi-model is considered as the average (ENSEMBLE) of the seven models in GCMs and RCMs.

For both climate models, monthly data of air temperature (max and min), relative humidity, wind speed and solar radiation are used to estimate evapotranspiration in three periods. Indeed, the period 1984–2000 is used to assess the performance of climate models against reanalyses for estimating ET_0 by the Penman-Monteith method (Allen et al., 1998). This assessment only concerns the historical period of climate models (1984–2000). The period 1984–2000 is used not only because of the length of the data series available but also to have a homogeneous period for reanalyses and climate models. For the same reason of data availability, the historical period is 1971–2000 and the projection one is 2036–2065. The annual and seasonal ET_0 are obtained by summing monthly ET_0 values. For climate variables, the averages values are used. Two seasons are considered: a dry season (November to May) and a rainy season (June to October) even though, the length of the seasons varies according to the climatic zones of the basin (Ndiaye et al., 2020b). The coordinates of 31 OMVS weather stations and 33 virtual stations (Fig. 1, Ndiaye et al., 2020b) were used to extract both reanalyses and outputs of climate models.

2.3. Methodology

The methodology employed here consists of (i) the performance evaluation of reanalyses compared to observations, (ii) the performance evaluation of the GCMs and RCMs compared to the reanalyses for the estimation of reference evapotranspiration (ET_0) over the period 1984–2000, (iii) evaluation of the change of ET_0 and climate variables between the periods 1971–2000 and 2036–2065, (iv) the sensitivity analysis of ET_0 to climatic variables and detection of the trends of ET_0 and climate variables over the period 2036–2065.

2.3.1. Performance evaluation of reanalyses data

Due to the lack of sufficient climate observations in the Senegal River Basin, reanalyses data were used here. The meteorological variables extracted from the NASA databases were first evaluated against ground based observations, to establish their temporal consistency and verify if they reproduce the same trend.

For this, we chose the stations which have at least three meteorological variables available on a daily scale. These are the stations of Kayes, Kita, Nioro du Sahel and Bamako Senou. These four stations cover the range of climatic zones found in the Senegal River basin (Fig. 1b). For each station, for the sake of better legibility of the results, a single year was chosen to represent the trend of climatic variables. To evaluate the agreement between the reanalyses and the observed data, the Kling Gupta Efficiency (Gupta et al., 2009) is used (Eq. 2). In order to take into account the climate zones (sahelian, sudanian and guinean) of the basin, two stations (Labe and Mamou) are added to the four previous ones for assessing the KGE.

Table 1
Characteristics of GCMs and RCMs used.

Institute	GCMs names	GCMs Resolution (Lat × Long)	RCMs names	RCMs Resolution (Lat × Long)
Canadian Center of Climate Modelling and Analysis	CANESM2	2.77° × 2.81°	CANESM2.RCA4	0.44°× 0.44°
NOAA Geophysical Fluid Dynamics laboratory	GDFL-ESM2M	2.5° x 2.01°	GFDL-ESM2M. RCA4	0.44°× 0.44°
Met Office Hadley Center	HadGEM2-ES	1.25° × 1.87°	HadGEM2-ES. RCA4	0.44°× 0.44°
Centre National de Recherche Météorologique-Groupe d'étude de l'Atmosphère Météorologique and Centre Européen de Recherche et de Formation Avancée	CNRM-CM5	1.39° × 1.40°	CNRM-CM5. RCA4	0.44°× 0.44°
National Institute for Environmental Studies, and Japan Agency for Marine-Earth Science and Technology	MIROC5	1.40° × 1.40°	MIROC5.RCA4	0.44°× 0.44°
Institut Pierre-Simon Laplace	IPSL-CM5A-MR	1.25°x2.5°	IPSL-CM5A-MR. RCA4	0.44°× 0.44°
Commonwealth Scientific and Industrial Research Organization	CSIRO-MK3−6-0	1.87° × 1.87°	CSIRO-Mk3−6-0.RCA4	0.44°× 0.44°

2.3.2. Evaluating the performance of climate model projections

The performance of climate models' projections is assessed in two steps. First, the difference between the yearly average of ET_0 of reanalyses and that of GCMs and RCMs is assessed over the period 1984–2000 by using the following equation:

$$\Delta ET_{0rea-model} = \frac{1}{n}\sum(ET_{0model} - ET_{0rea}) \quad (1)$$

Where $\Delta ET_{0rea-model}$ is the difference between ET_0 of reanalyses and models, ET_{0rea} is the ET_0 calculated with reanalyses data, ET_{0model} is ET_0 calculated with GCMs and RCMs and n the length of the series.

Then, the Kling Gupta Efficiency (KGE-Gupta et al., 2009) and the Percentage of Bias (PBIAS) are used as evaluation criteria at monthly scale. The KGE combines the correlation coefficient (r), the biases (β) and the variability (α). It varies from -∞ to 1 and its optimal value is 1. The formulation of the KGE is as follows:

$$KGE = 1 - \sqrt{(r-1)^2 + (\beta-1)^2 + (\alpha-1)^2} \quad (2)$$

Percent bias (PBIAS) indicates the underestimation / overestimation of ET_0 by climate models. It varies from -∞ to + ∞ and its optimal value is 0. Its formulation is as follows:

$$PBIAS = \left[\frac{\frac{1}{n}\sum_{i=1}^{n}(ET_{ocm} - ET_{0rea})}{\frac{1}{n}\sum_{i=1}^{n}(ET_{ocm})}\right] * 100 \quad (3)$$

Where, ET_{ocm} is the reference evapotranspiration estimated from the climate models, ET_{0rea} is the ET_0 estimated by the reanalysis and n is the length of the data.

2.3.3. Sensitivity analysis and calculation of the rate of change

The sensitivity analysis allows to determine the impact of climate variables on the reference evapotranspiration (Zhao et al., 2014). The influence of each variable is determined by calculating a sensitivity coefficient. Its wording is as follows:

$$S_{vi} = \frac{\partial ET_0}{\partial_{vi}} \times \frac{vi}{ET_0} \quad (4)$$

Where, S_{vi} is the sensitivity coefficient, ∂ET_0 variation of the reference evapotranspiration (ET_0) caused by the change of a variable ∂_{vi}, is the considered variable. A positive (negative) sensitivity coefficient indicates that the variable causes an increase (decrease) in ET_0. The higher the absolute value of the sensitivity coefficient, the more influence the variable has on ET_0 (Li et al., 2017).

The rate of change of ET_0 is calculated between the mean of ET_0 on the historical period (1971–2000) and the projections (2036–2065) according to the following formula:

$$RC = \frac{ET_{0Pro} - ET_{0Hist}}{ET_{0Hist}} \times 100 \quad (5)$$

Where, RC is the rate of change in %, ET_{0Hist} is the mean reference evapotranspiration calculated over the historical period and ET_{0Pro} is the mean reference evapotranspiration calculated in the future. A positive (negative) value for the rate of change indicates an increase (decrease) in evapotranspiration in the future. The same Eq. (4) is used for calculating the rate change of climate variables.

2.3.4. Trend in reference evapotranspiration and climatic variables

The Mann Kendall test (Mann, 1945; Kendall, 1975) is used to detect the trend of annual and seasonal ET_0 and climate variables on the period 2036–2065 according to the RCP4.5 and RCP8.5 scenarios. The Mann Kendall test is based on two hypotheses: hypothesis (denoted H0) which assumes that the series is stationary, without trend and the alternative hypothesis (H1) which indicates the existence of a trend by rejecting H0. A positive/negative trend is obtained from the +/- sign of the Z value of the Mann Kendall test. The trend obtained is measured by its degree of significance, that is to say the probability associated with the rejection or not of the null hypothesis. The significance level used in this study is 0.05. When $|Z| > 1.96$ the null hypothesis is rejected and the trend is significant at 5%. The amplitude of the trend is measured by the slope of Sen (Sen, 1968) denoted (β).

The method of interpolation of the Inverse Distance Weighting (IDW) (Chu et al., 2017) is used to spatialize the ET_0 and climate variables on an annual and seasonal scale. The IDW interpolation technique is widely used to analyze the spatial distribution of evapotranspiration (Qi et al., 2017; Malamos et al., 2017; Ndiaye et al., 2020b).

3. Results and discussion

3.1. Performance of reanalyses against observed data

The climate variables available for the four weather stations (Bamako Senou, Kayes, Kita and Nioro du Sahel) are maximum and

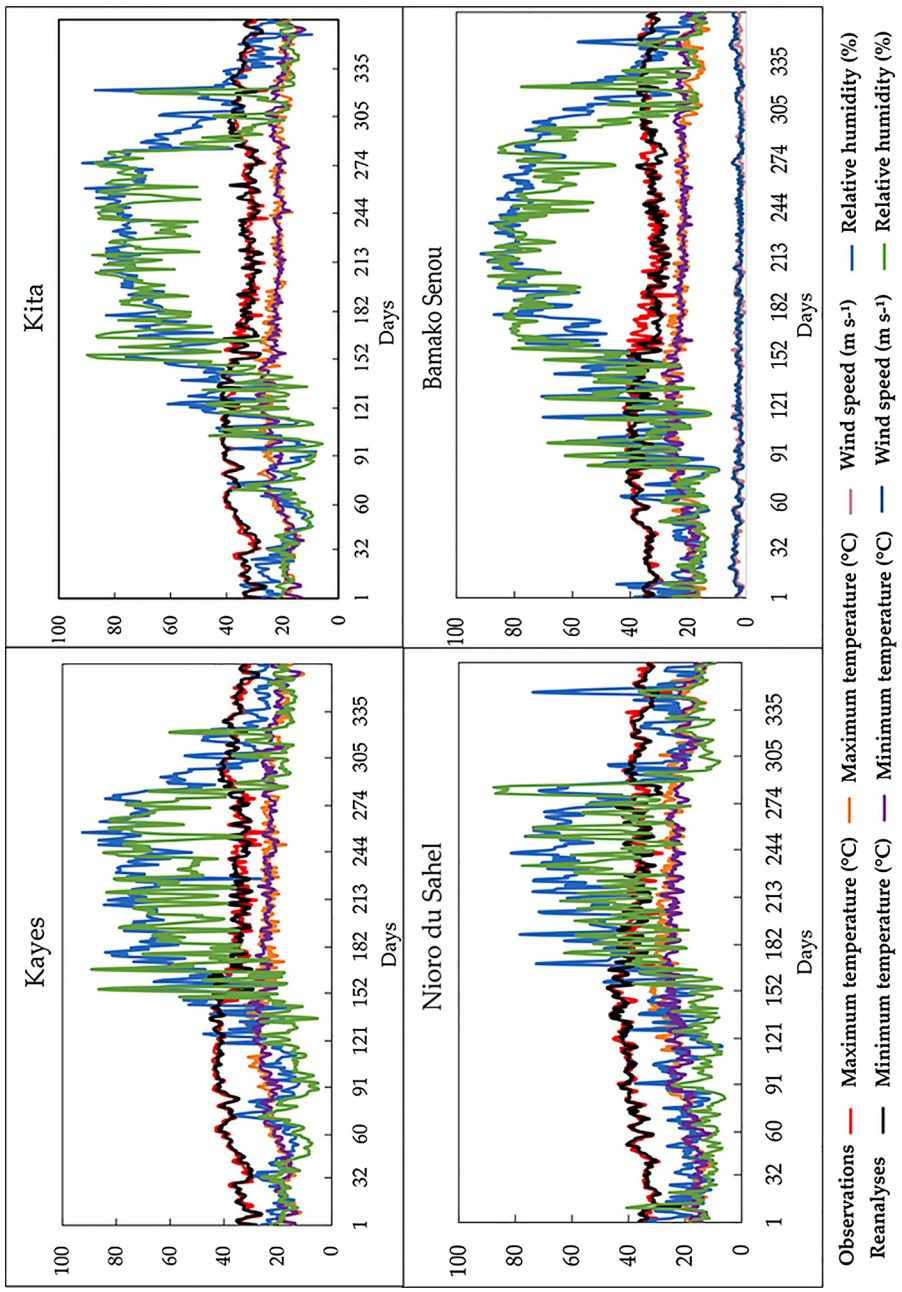

Fig. 2. Temporal consistency of observed climatic variables and those of reanalyses.

minimum temperature, relative humidity and wind speed. The latter is only available for Bamako Senou weather station. The temporal consistency between observed data and reanalyses is shown in Fig. 2 for a given year. Table 2 provides the KGE values and its components (r, alpha, beta) according to climate variables available and climate zones. Fig. 2 shows good consistency for Tmax, Tmin, and lesser for Rh. Table 2 confirms good performance for Tmax with KGE above 0.5 for all stations. KGE for Tmin is also high, except on Guinean stations. This may be explained by the coarse resolution of reanalyse data and the fact that their reliability appears to vary with the location, time period and variables considered (Martins et al., 2016). For Rh, despite some variability in Fig. 2, KGE remains high. Wind speed KGE values are much lower around 0.2 but Fig. 2 shows relative agreement in the overall amplitude of the wind.

Overall, these results show acceptable consistency between the observed data and the reanalyses for the key climatic variables at the Kayes, Kita, Nioro du Sahel and Bamako Senou stations. Accordingly, the reanalyses were used as reference here for assessing the performance of climate models.

3.2. Performance of GCMS and RCMs against reanalyses data

Fig. 3 shows the spatial distribution of the difference in the annual ET_0 of climate models and reanalyses over the period 1984–2000. Results show that the difference in annual ET_0 between reanalyses and GCMs varies from -1560 to +820 mm depending on the models (Fig. 3). The maximum negative values are obtained by IPSL-CM5A-RC and CSIRO-MK3−6-0 models in Sahelian and Sudanian climate zones. For the ENSEMBLE average of all models, the difference ranges from -747 to +283 mm. individually, the HADGEM, CNRM, and CANESM models exhibit ET_0 values closer to reanalyses. RCMs, on the other hand, show ET_0 values that are closer to reanalyses compared to GCMs. However, they generally tend to overestimate evapotranspiration, while GCMs here tend to underestimate it. For example, the difference in annual ET_0 between reanalyses and regional models ranges from -483 to +1110 mm depending on the model. The ENSEMBLE average of all regional models shows a difference ranging from -139 to +720 mm (Fig. 4). The ET_0 values of the regional models CANESM2.RCA4, CNRM-CM5.RCA4 and HadGEM2-ES.RCA4 are closer to those obtained with reanalyses.

Overall, the results show that the differences between ET_0 values from reanalysis data and climate models are relatively high. This may be explained by the difficulty of climate models to reproduce correctly the climate variables used for estimating reference evapotranspiration. Indeed, the ET_0 values obtained from reanalyses are closer to those of Bodian (2011) and Djaman et al. (2015) in Senegal River Basin. According to Bodian (2011), at Labé and Siguiri (Guinean zone) weather stations, the observed values of ET_0 were 1611 mm and 1969 mm over the period 1960−1996. For these two stations, the values of reanalyses are 1838 mm and 1936 mm over the period 1984–2017. Moreover, in Sahelian zone, Djaman et al. (2015) used the observed data of Africa Rice Center research stations at Ndiaye and Fanaye (Sahelian Regional station, Senegal) for estimation reference evapotranspiration over February 2013 and May 2014. They showed that reference evapotranspiration varies from 1 to 14 mm/day with an average of 6 mm/day (2190 mm/year) at Ndiaye and from 3 to 18 mm/day with an average of 10 mm/day (3650 mm/year) at Fanaye. For the reanalyses, ET_0 varies between 1–18 mm/day with an average of 8 mm/day (2920 mm/year) over the period 1984–2017 at Fanaye.

Figs. 4 and 5 respectively give the spatial distribution of KGE and PBIAS and Fig. 6 gives a synthesis of KGE and PBIAS as a function of climatic zones. For the GCMs, the KGE vary from -0.35 to 0.68. The highest values are obtained by the CANESM2 and GDFL-ESM2M models and the lowest by CSIRO-MK3−6-0 and HadGEM2-ES. The biases vary from -124 % to 38 %. The mean values of PBIAS show that GCMs underestimate evapotranspiration in 91 % of stations in the basin. The average of all GCMs shows KGE values of 0.09 to 0.48 and biases of -58 % to 24 %. From a spatial point of view, the results are almost similar depending on the climatic zones. From the Guinean zone to the Sahelian one, the GCMs have KGE of less than 0.60 and underestimate the evapotranspiration. These results obtained show that GCMs are less robust for the estimation of evapotranspiration. This can be explained by the coarse resolution of the

Table 2
KGE values for the four selected weather stations.

Weather stations	Climate zones	Climate variables	Periods	r	α	β	KGE
Bamako Senou	Sudanian	Tmax	2002−2003	0.66	0.99	0.99	0.66
		Tmin	2002−2003	0.58	0.8	1.06	0.53
		Rh	2002−2003	0.84	1.04	0.84	0.77
		u2	2002−2003	0.24	1.19	1.23	0.19
Kayes	Sudanian	Tmax	1984−1996	0.6	1.06	0.98	0.59
		Tmin	1984−1996	0.71	0.78	1.01	0.63
		Rh	1984−1996	0.83	1.19	0.81	0.68
Kita	Sahelian	Tmax	1984−1987	0.8	1.11	0.99	0.77
		Tmin	1984−1987	0.75	0.85	1	0.71
		Rh	1984−1987	0.88	1.19	0.85	0.73
Nioro du Sahel	Sahelian	Tmax	2002−2003	0.76	1.04	1	0.75
		Tmin	2002−2003	0.8	0.79	0.95	0.71
		Rh	2002−2003	0.76	0.88	0.67	0.57
Labé	Guinean	Tmax	1986−1996	0.69	1.33	1.07	0.54
		Tmin	1986−1996	0.26	0.67	1.41	0.09
Mamou	Guinean	Tmax	1984−1998	0.75	1.26	1.01	0.64
		Tmin	1984−1998	0.30	0.79	1.19	0.25

Read: Tmax maximum temperature, Tmin minimum temperature, Rh Relative humidity, u2 wind speed.

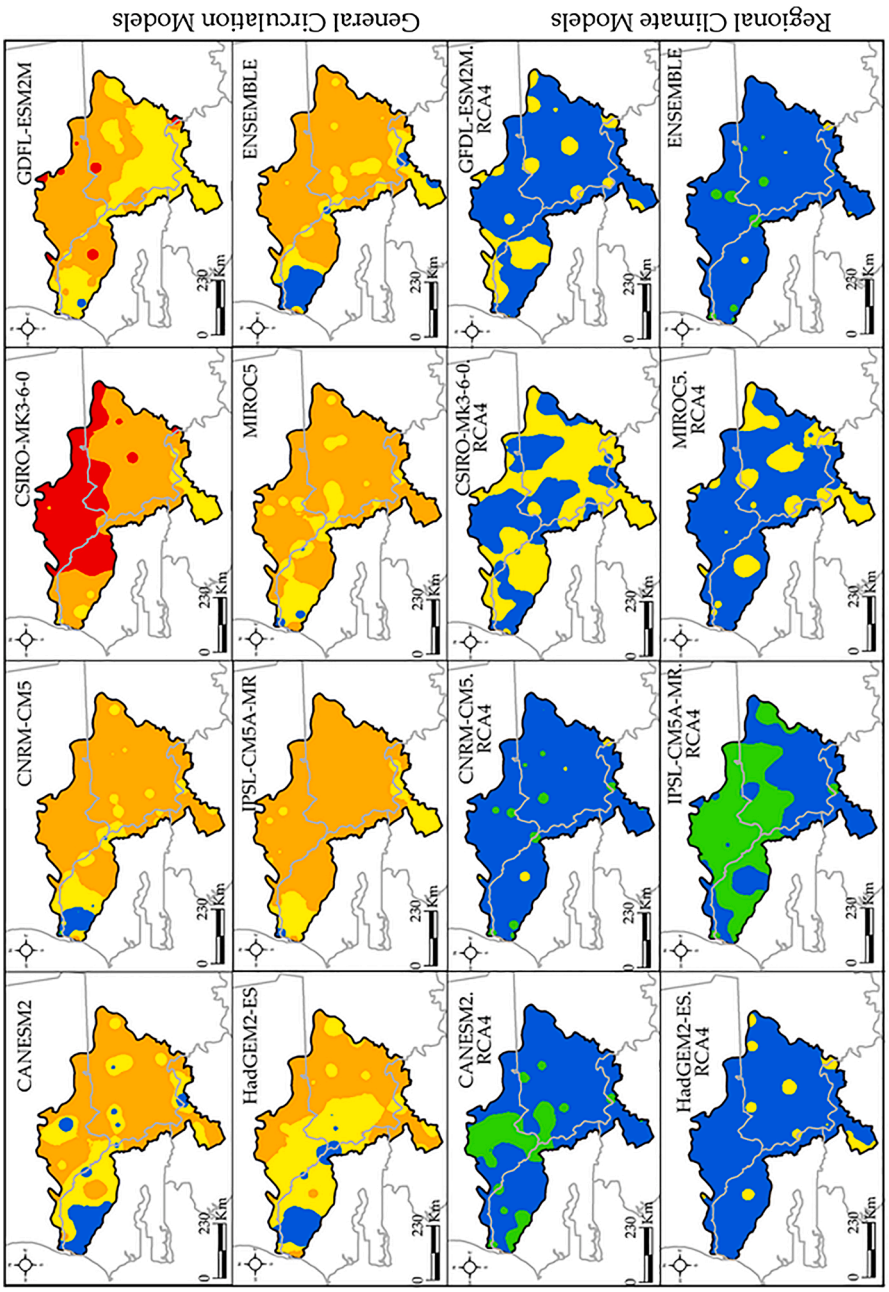

Fig. 3. Difference between annual average of ET_0 calculated by reanalyses and GCMs & RCMs models over the period 1984-2000.

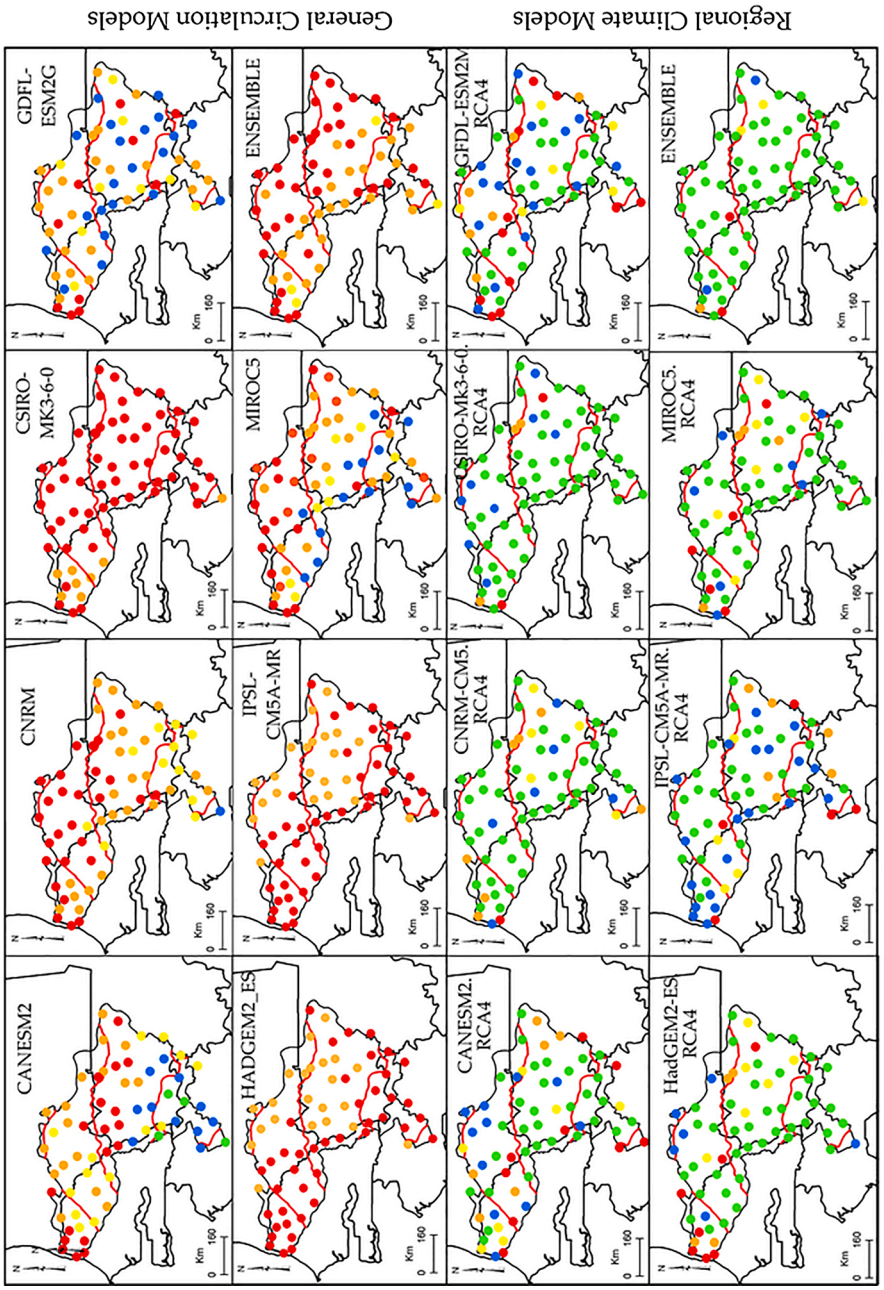

Fig. 4. Spatial distribution of the KGE for monthly ET_0 between climate models and reanalyses over the period 1984 – 2000.

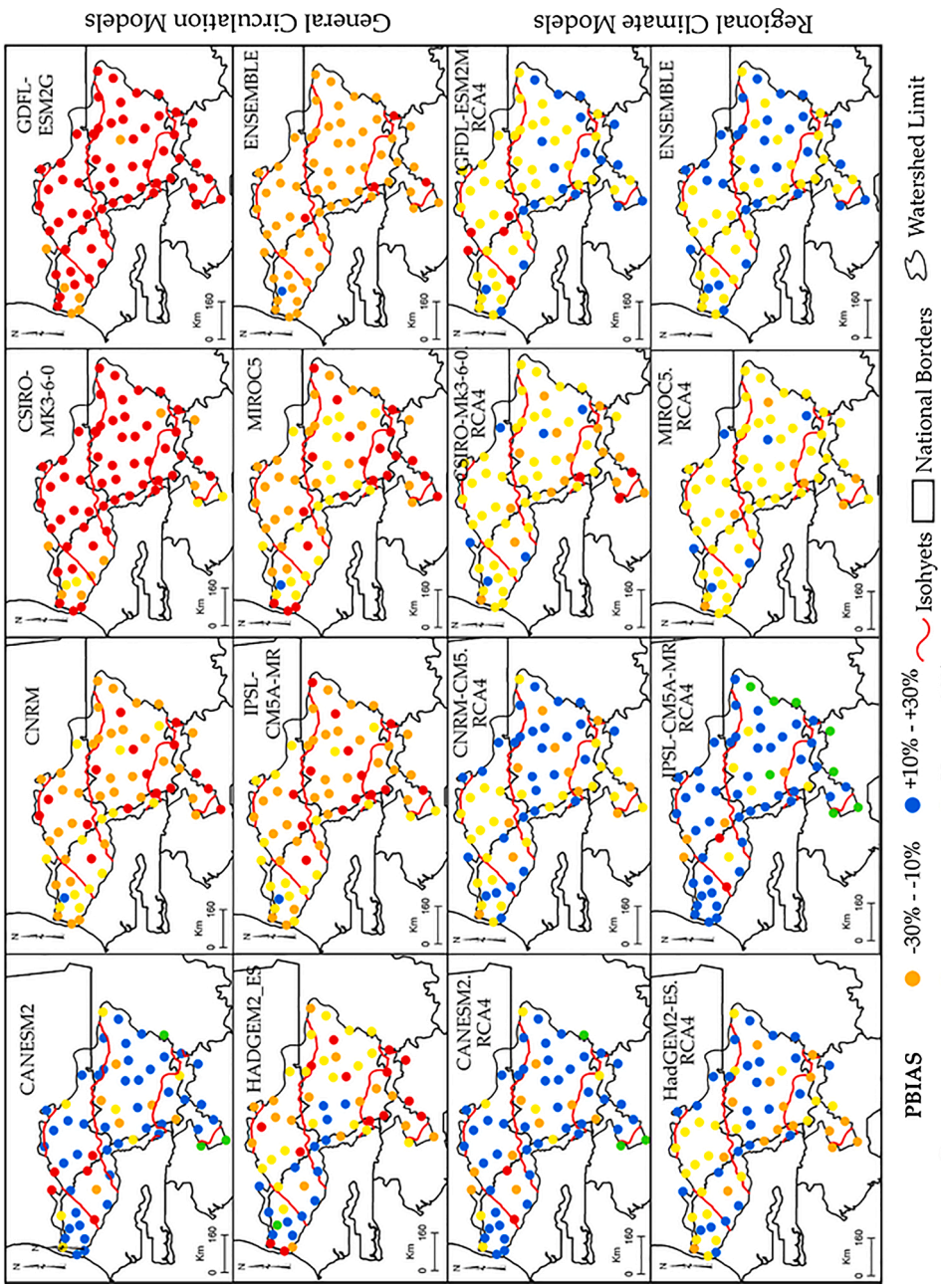

Fig. 5. Spatial distribution of PBIAS for monthly ET_0 between climate models and reanalyses over the period 1984–2000 (negative values indicate underestimation and positive one's overestimation).

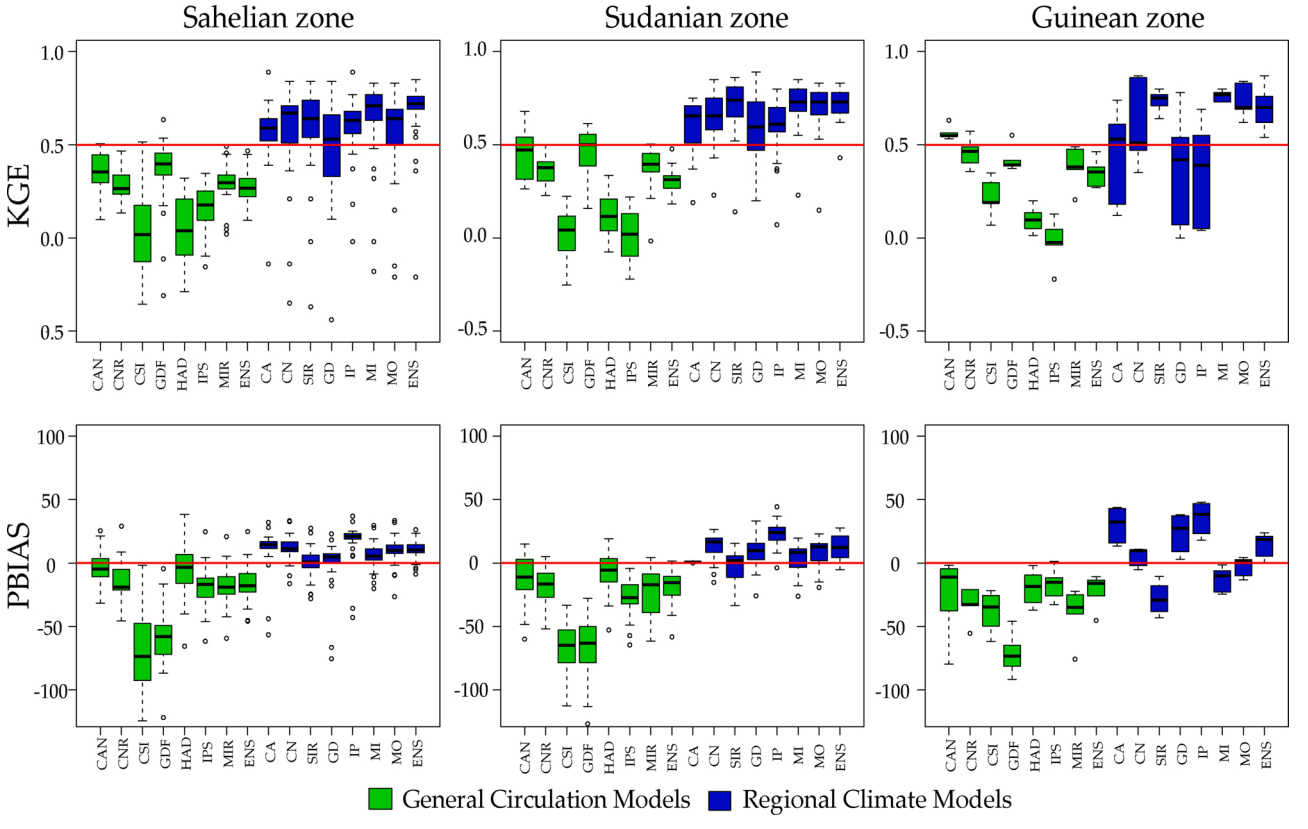

Fig. 6. KGE and PBIAS between climate models and reanalyses at monthly scale (CAN : CANESM2, CNR : CNRM, CSI : CSIRO-MK3-6-0, GDF : GDFL-ESM2G, HAD : HADGEM2-ES, IPS : IPSL-CM5A-MR, MIR : MIROC5, CA : CANESM2.RCA4, CN : CNRM-CM5.RCA4, SIR : CSIRO-Mk3-6-0.RCA4, GD : GFDL-ESM2M.RCA4, IP : IPSL-CM5A-MR.RCA4, MI : MIROC5.RCA4, MO : HadGEM2-ES.RCA4, ENS : ENSEMBLE).

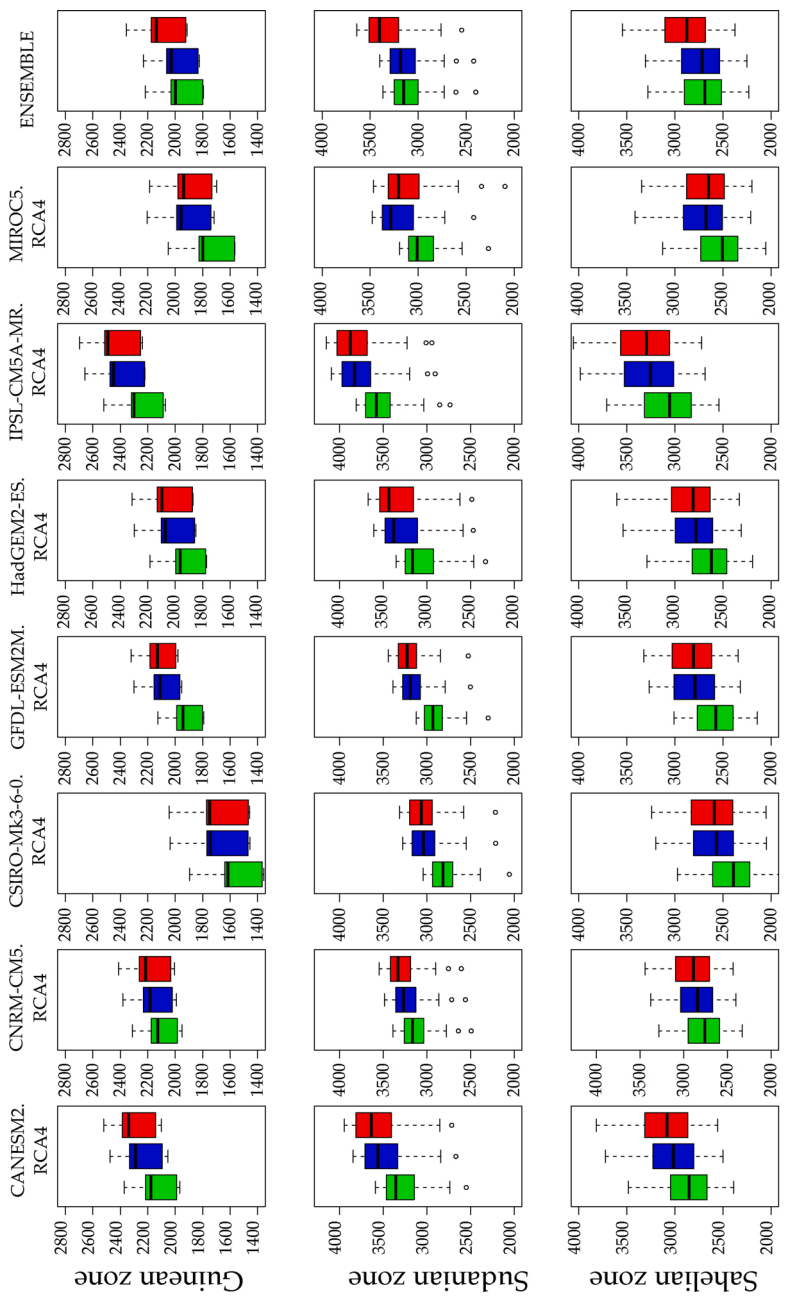

Fig. 7. Annual average of evapotranspiration (mm) on historical and projection periods.

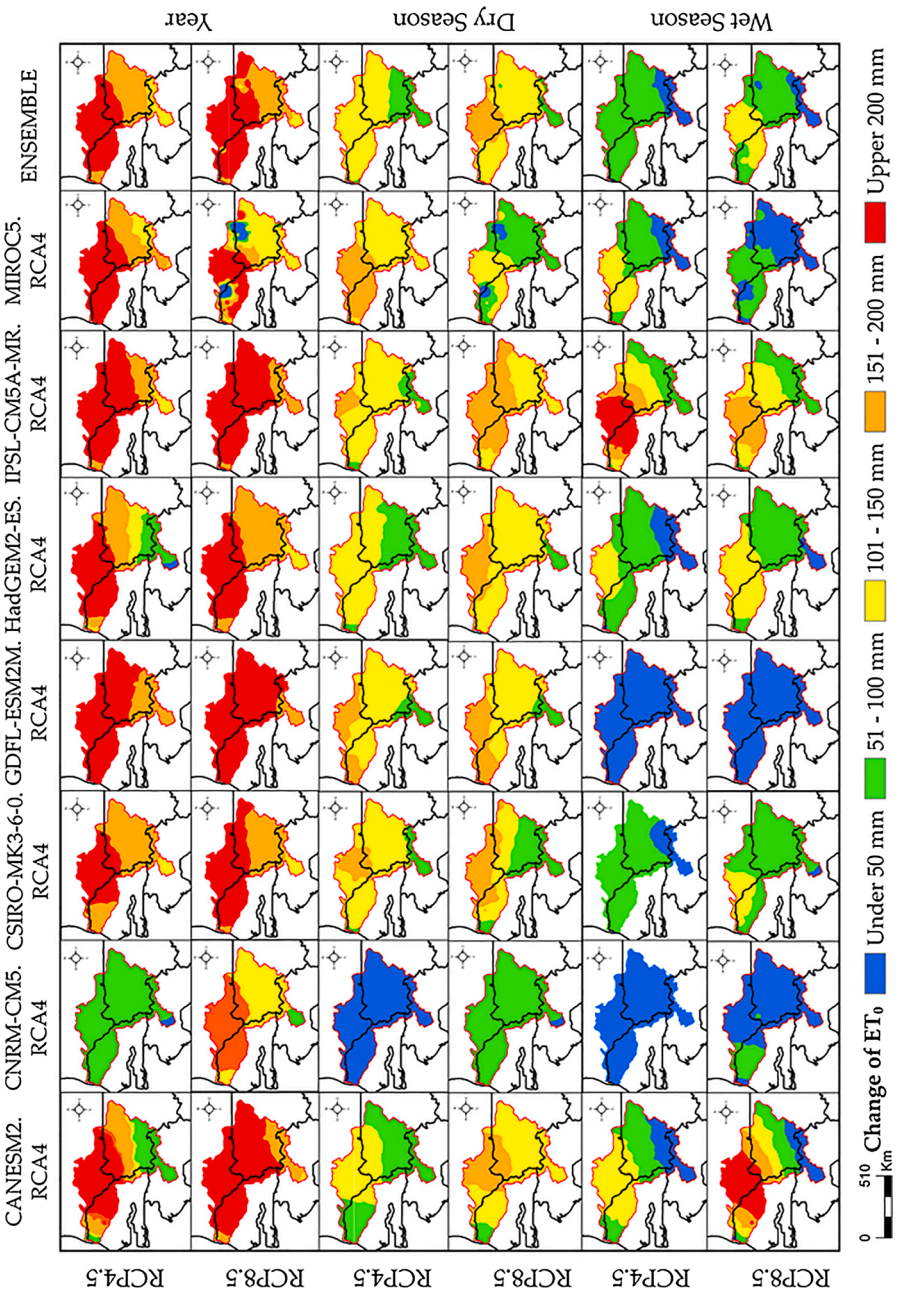

Fig. 8. Spatial distribution of change of the ET_0 of the RCMs calculated between the historical period 1971-2000 and that of the 2036-2065 projections.

GCMs and their uncertainty in estimating the climate variables necessary for the estimation of evapotranspiration.

Fig. 4 shows that the KGE of RCMs are greater than 0.60 in the most of the stations and are more in agreement with the reanalyses than the GCMs. The average KGE and PBIAS of the regional models vary from -0.21 to 0.87 and from -8% to 27 % respectively. Unlike GCMs, RCMs overestimate ET_0 at 88 % of stations. From a spatial point of view, the mean KGE values of multi-models ENSEMBLE are 0.70 (min and max vary from 0.54 to 0.87) in Guinean zone, 0.72 (0.43 to 0.83) in Sudanian area and 0.67 (0.36 to 0.85) in the Sahelian zone. The PBIAS show that all RCMs overestimate evapotranspiration in all climate zones, with the exception of CSIRO-Mk3−6-0.RCA4 and MIROC5RC.RCA4 which underestimate it in the Guinean zone. Moreover, some regional models have better performances than the ENSEMBLE average of all models in some climate zones. For example, in Guinean zone, the KGE values of CSIRO-Mk3−6-0.RCA4, HadGEM2-ES.RCA4 and MIROC5RC.RCA4 are respectively 0.73, 0.74 and 0.76 and that of the ENSEMBLE average models is 0.70. However, in Sahelian and Sudanian zones, the ENSEMBLE performs better than the individual models.

Overall, RCMs are more robust than GCMs for estimating evapotranspiration in the Senegal River basin. For this purpose, only RCMs will be taken into account in subsequent analyses. The reanalyses data used to perform climate models seem coherent with observed data used by Bodian (2011) and Djaman et al. (2015) in the High Basin and the Valley of Senegal River. Moreover, the different values of KGE and PBIAS obtained by the models in the climate zones may be explained by the structure of the models, the heterogeneity of the landscape and the number of stations used in each climate zones. For example, in Guinean zone (1% of the basin) only the mean values of five stations are analyzed against 33 and 26 stations in Sudanian (37 %) and Sahelian zones (62 %), respectively. The reanalyses used as a reference are not validated by observed data; which can influence the calculation of the rate of reference evapotranspiration. The difficulty of climate models in correctly simulating the variables necessary for estimating ET_0 would also be a source of uncertainty.

3.3. Change in evapotranspiration by 2065

All the models agree on a positive variation in evapotranspiration on the period 2036–2065. Fig. 7 shows mean values of annual evapotranspiration in both historical and projection periods according to the climate zones. Fig. 8 gives the spatial distribution of the ET_0 change at annual and seasonal scales. In the Guinean zone, the minimum and maximum values of annual ET_0 vary from 1355 to 2521 mm on the period 1971–2000 according to climate models. During the period 2036–2065, these values vary from 1455 to 2657 mm for RCP4.5 and 1457–2696 mm for RCP8.5. The maximum values were obtained by IPSL-CM5A-MR.RCA4. The increase of ET_0 in the Guinean zone varies from 14 to 173 mm (i.e. 2–11%) for RCP4.5 and from 55 to 196 mm (i.e. 2.4–11%) for RCP8.5 according to the models. In Sudanian zone, the ET_0 values vary from 1902 to 2390 mm over the period 1971–2000. The ET_0 for the period 2036–2065 vary from 2046 to 2386 for RCP4.5 and 2051–4056 mm for RCP8.5. This means that, according to the models, ET_0 will increase by 2–9% (56–285 mm) for RCP4.5 and 4–11% (99–365 mm) for RCP8.5 until 2065. The ET_0 values will reach 4095 mm for RCP4.5 and 4153 mm for RCP8.5 compared to the period 1971–2000 where the maximum value of ET_0 was 3810 mm in the Sahelian zone. The increase of ET_0 varies between 3–10 % (63 and 293 mm) for RCP4.5 and 3–12 % (106−387 mm) for RCP8.5. Moreover, it is interesting to note that among the models, MIROC5.RCA4 shows higher values of ET_0 for RCP4.5 than RCP8.5 in the three climate zones. This surprising result may be explained by the interactions between local climatic processes and the reduced maximum temperature and wind speed modelled by this RCMs under scenario RCP8.5 (Section 3.4.2). At the seasonal scale, the models show that, until 2065, evapotranspiration will increase during the dry and wet season. For example, in the Sahelian zone, the ET_0 will increase between 27 and 181 mm (2–9 %) for RCP4.5 and 72−189 mm (4–10 %) for RCP8.5. In the Guinean and Sudanian zones the maximum values of ET_0 will respectively reach 123–150 mm for RCP4.5 and 128−176 mm for RCP8.5. During the rainy season, ET_0 will increase at a rate of 0–18 % in Sahelian and Sudanian zones according to the models and the two scenarios. It will increase from 3 to 15 % in the Guinean zone.

Overall, according to the RCMs, the ET_0 will continue to increase until 2065 in Senegal River Basin. Similar results have been obtained in different regions of the world. Thus, Obada et al. (2017) noted that all three models they used project an increase in ET_0 from 3% to 10.91 % in Benin (West Africa) over the period 2041−2070. In a semi climate arid in Spain, Giménez and García-Galiano (2018) predict an increase in ET_0 from 4.42 % to 16.21 % by 2050, compared to the average for the period 1960−1990. The increase in ET_0 by 2050 could be accompanied by a decrease in flows. Indeed, according to Bodian et al. (2018), compared to the period 1971–2000, the annual flows of the Bafing, the main tributary of the Senegal River, will decrease by 8% according to the RCP4.5 scenario and by 16 % under RCP8.5 scenario by 2050 in West Africa. This means that the annual flows depend on precipitation variability and evapotranspiration. The continued increase of the latter may affect the water resources and exacerbate competition between users. Moreover, it is important to note that Ndiaye et al. (2020b) highlighted a significant decrease of evapotranspiration in the Sahelian zone and mentioned the existence of an "evaporation paradox" in the Senegal River Basin on the period 1987−2017. However, no model has highlighted a significant decrease of evapotranspiration on the period 2036–2065. Therefore the "evaporation paradox" will not exist on the period 2036–2065 according to the RCMs.

3.4. Sensitivity of future evapotranspiration to climatic variables

The influence of climatic variables on evapotranspiration is determined by calculating a sensitivity coefficient. Thus, Fig. 9 gives the spatial distribution of the annual sensitivity coefficients according to the models and Table 2 indicates the average values of the coefficients according to climatic zones. With the exception of relative humidity, all variables have positive sensitivity coefficients. In other words, their increase leads to an increase in evapotranspiration.

Table 3 shows that the relative humidity sensitivity coefficients vary from -0.90 to -8. from -0.90 to -8.4 depending on the models,

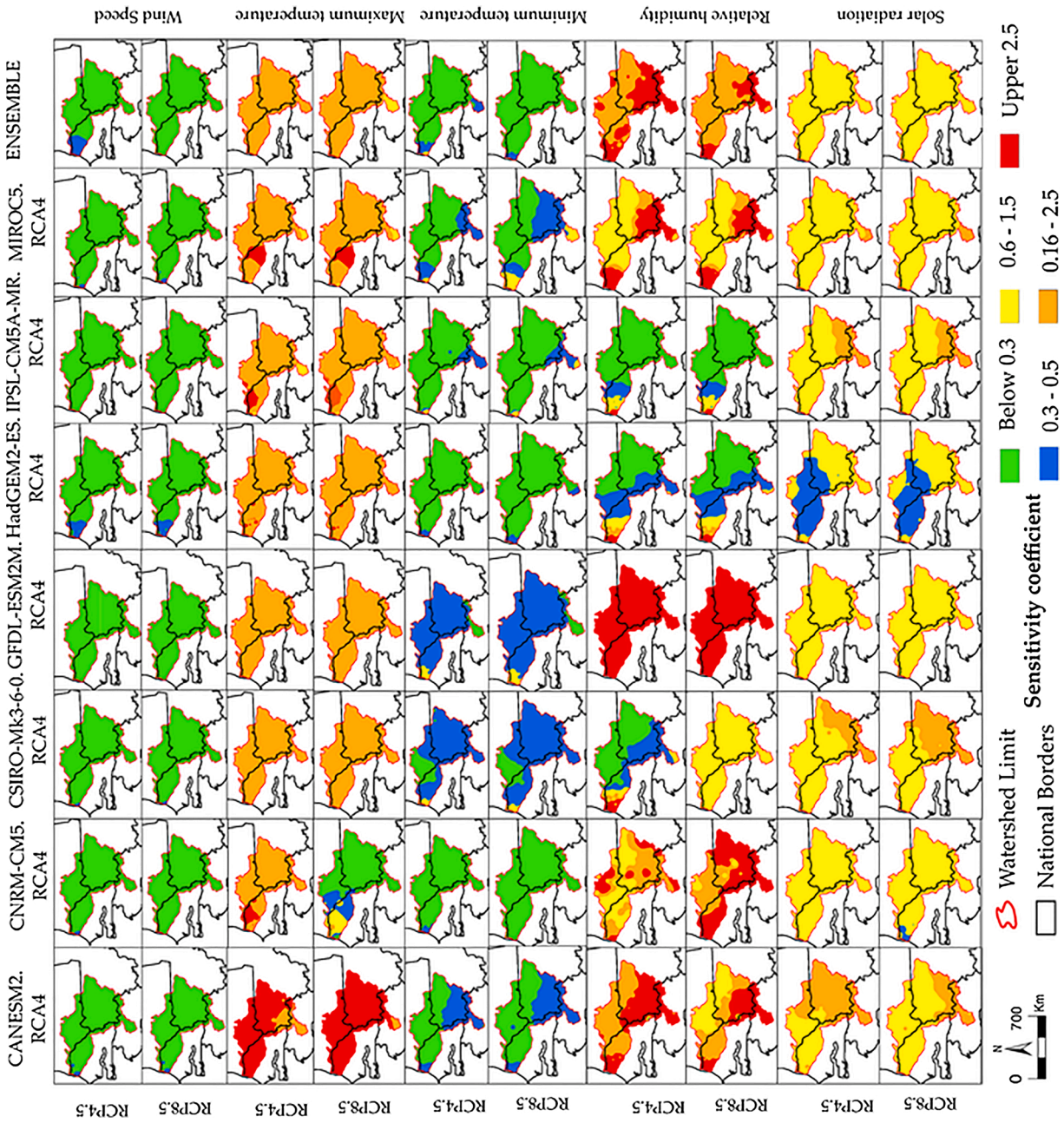
CANESM2. RCA4
CNRM-CM5. RCA4
CSIRO-Mk3-6-0. RCA4
GFDL-ESM2M. RCA4
HadGEM2-ES. RCA4
IPSL-CM5A-MR. RCA4
MIROC5. RCA4
ENSEMBLE
Solar radiation
Relative humidity
Minimum temperature
Maximum temperature
Wind Speed
RCP8.5
RCP4.5
Watershed Limit
National Borders
Sensitivity coefficient
Below 0.3
0.3 - 0.5
0.6 - 1.5
0.16 - 2.5
Upper 2.5
N
0
700
Km

Fig. 9. Spatial distribution of the sensitivity coefficients of ET_0 to climate variables of regional models at the annual scale over the period 2036-2065.

under both the RCP4.5 and RCP8.5 scenarios. The maximum values of relative humidity are observed in the Guinean zone and those minimum in the Sahelian zone. The maximum temperature coefficients range from 1.35 to 2.59 under RCP4.5 and from 1.35 to 2.49 under RCP8.5. The influence of maximum temperature on evapotranspiration is greater in the Sahelian and Sudanian areas. Solar radiation is the third variable that has the most influence on ET_0 with coefficients varying from 0.60 to 0.97 under the two scenarios. Its maximum values are noted in the Guinean zone. Wind speed and minimum temperature have less influence on ET_0 with coefficients below 0.35. Wind speed has more influence on ET_0 in the Sahelian and Sudanian areas. The results obtained confirm those of Ndiaye et al. (2020b) who noted that evapotranspiration is more sensitive to relative humidity, maximum temperature and solar radiation in the Senegal River basin over the period 1984–2017.

On a seasonal scale, relative humidity, maximum temperature and solar radiation are always the variables that have the most influence on evapotranspiration. The influence of relative humidity on ET_0 is more significant during the rainy season and in the Guinean zone with coefficients varying from -0.86 to -3.49 under RCP4.5 and from -8.07 to -15.36 under RCP8. 5. ET_0 is more sensitive to maximum temperature during the dry season and in the Sudanese and Sahelian areas. Solar radiation has more influence on ET_0 in the Guinean area and during the rainy season.

The sensitivity analysis shows that future evapotranspiration will be more influenced by relative humidity, maximum temperature and solar radiation. Therefore, it would be important to pay more attention to the measurement and/or estimation of these climatic variables in order to ensure a good estimate of evapotranspiration. It is also important to note that the climate variable influence on ET_0 depend on climate zones. The influence of relative humidity and solar radiation is more significant in Guinean zone than in Sahelian and Sudanian ones. However, in Sudanian and Sahelian zones, the ET_0 is most sensible to maximum temperature, minimum temperature and wind.

3.5. Is the climate stationary in 2036–2065?

3.5.1. Future trends in evapotranspiration

The spatial distribution of Mann Kendall's Z of annual and seasonal evapotranspiration on the period 2036–2065 is given in Fig. 10. The average of all regional models shows a significant increase ($p < 0.05$) in annual and seasonal ET_0 over the entire basin according to the RCP4.5 and RCP8.5 scenarios. The HadGEM2-ES.RCA4, IPSL-CM5A-MR.RCA4, CSIRO-Mk3−6-0.RCA4 and CANESM2.RCA4 models show a significant increase in annual evapotranspiration. For all the models, only GFDL-ESM2M.RCA4 shows a non-significant trend in annual and seasonal ET_0 over the entire basin. Fig. 11 shows the magnitude of the ET_0 trends depending on the models. In the Guinean zone, the annual ET_0 increases by 1.78 mm/year according to the RCP4.5 scenario and by 3.06 mm/year according to RCP8.5

Table 3
: Summary of the sensitivity coefficients of ET_0 to climate variables at the annual scale (CA : CANESM2.RCA4, CN : CNRM-CM5.RCA4, SIR : CSIRO-Mk3-6-0.RCA4, GD : GFDL-ESM2M.RCA4, IP : IPSL-CM5A-MR.RCA4, MI : MIROC5.RCA4, MO : HadGEM2-ES.RCA4, ENS : ENSEMBLE).

Climate zones	Modèles	Wind speed		Maximum temperature		Minimum temperature		Relative humidity		Solar radiation	
		RCP4.5	RCP8.5	RCP4.5	RCP8.5	RCP4.5	RCP8.5	RCP4.5	RCP8.5	RCP4.5	RCP8.5
Guinean	CA	0.23	0.22	1.87	1.69	0.30	0.25	−3.98	−3.86	0.91	0.91
	CN	0.23	0.23	1.63	1.63	0.22	0.22	−4.16	−4.16	0.87	0.87
	CS	0.21	0.21	1.35	1.35	0.33	0.33	−8.44	−8.44	0.88	0.88
	GD	0.24	0.24	1.53	1.53	0.24	0.24	−6.51	−6.51	0.80	0.80
	IP	0.23	0.23	1.78	1.78	0.25	0.25	−3.41	−3.41	0.94	0.94
	MI	0.21	0.21	1.48	1.48	0.31	0.31	−6.00	−6.00	0.97	0.97
	MO	0.22	0.22	1.56	1.56	0.27	0.27	−4.75	−4.75	0.94	0.94
	ENS	0.23	0.22	1.60	1.57	0.27	0.27	−5.32	−5.30	0.90	0.90
Sudanian	CA	0.26	0.25	2.43	2.23	0.26	0.22	−1.41	−1.45	0.75	0.77
	CN	0.25	0.25	2.13	2.13	0.20	0.20	−1.71	−1.71	0.83	0.83
	CS	0.23	0.23	1.94	1.94	0.31	0.31	−2.79	−2.79	0.88	0.88
	GD	0.26	0.26	2.02	2.02	0.23	0.23	−2.56	−2.56	0.78	0.78
	IP	0.26	0.26	2.35	2.35	0.21	0.21	−1.14	−1.14	0.75	0.75
	MI	0.24	0.24	1.98	2.05	0.36	0.29	−2.18	−2.18	0.92	0.92
	MO	0.25	0.25	2.10	2.10	0.25	0.25	−1.83	−1.83	0.85	0.85
	ENS	0.25	0.25	2.14	2.12	0.26	0.24	−1.95	−1.95	0.82	0.83
Sahelian	CA	0.32	0.31	2.59	2.38	0.24	0.21	−1.07	−1.12	0.60	0.63
	CN	0.30	0.30	2.27	2.27	0.20	0.20	−1.37	−1.37	0.70	0.70
	CS	0.28	0.28	2.12	2.12	0.32	0.32	−2.29	−2.29	0.81	0.81
	GD	0.30	0.30	2.13	2.13	0.25	0.25	−2.26	−2.26	0.70	0.70
	IP	0.32	0.32	2.49	2.49	0.19	0.19	−0.90	−0.90	0.60	0.60
	MI	0.29	0.29	2.23	2.21	0.28	0.27	−1.75	−1.90	0.76	0.71
	MO	0.30	0.30	2.26	2.26	0.23	0.23	−1.39	−1.39	0.69	0.69
	ENS	0.30	0.30	2.30	2.27	0.25	0.24	−1.58	−1.60	0.70	0.69

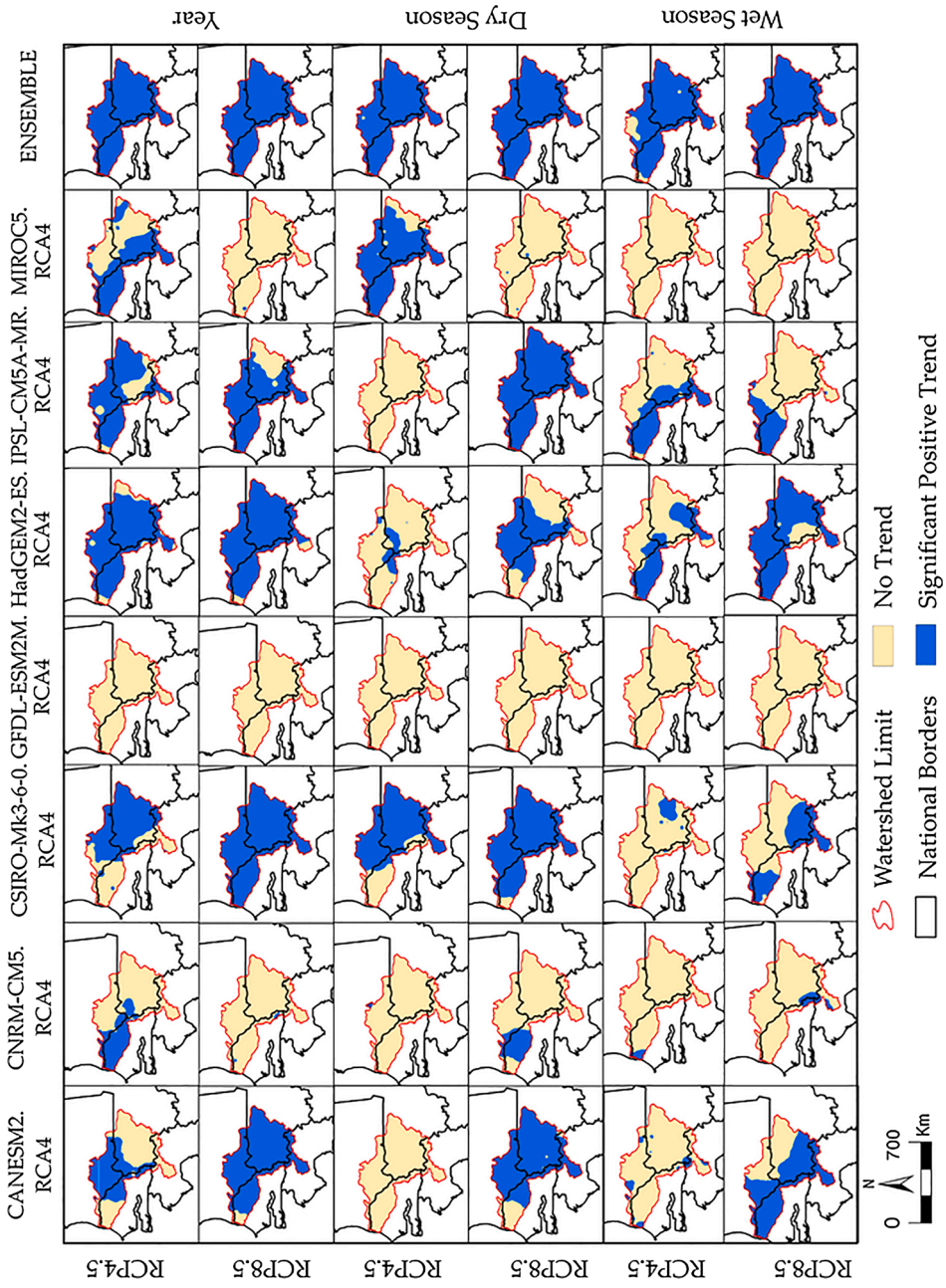

Fig. 10. Spatial distribution of Mann Kendall's Z of regional models over the period 2036–2065.

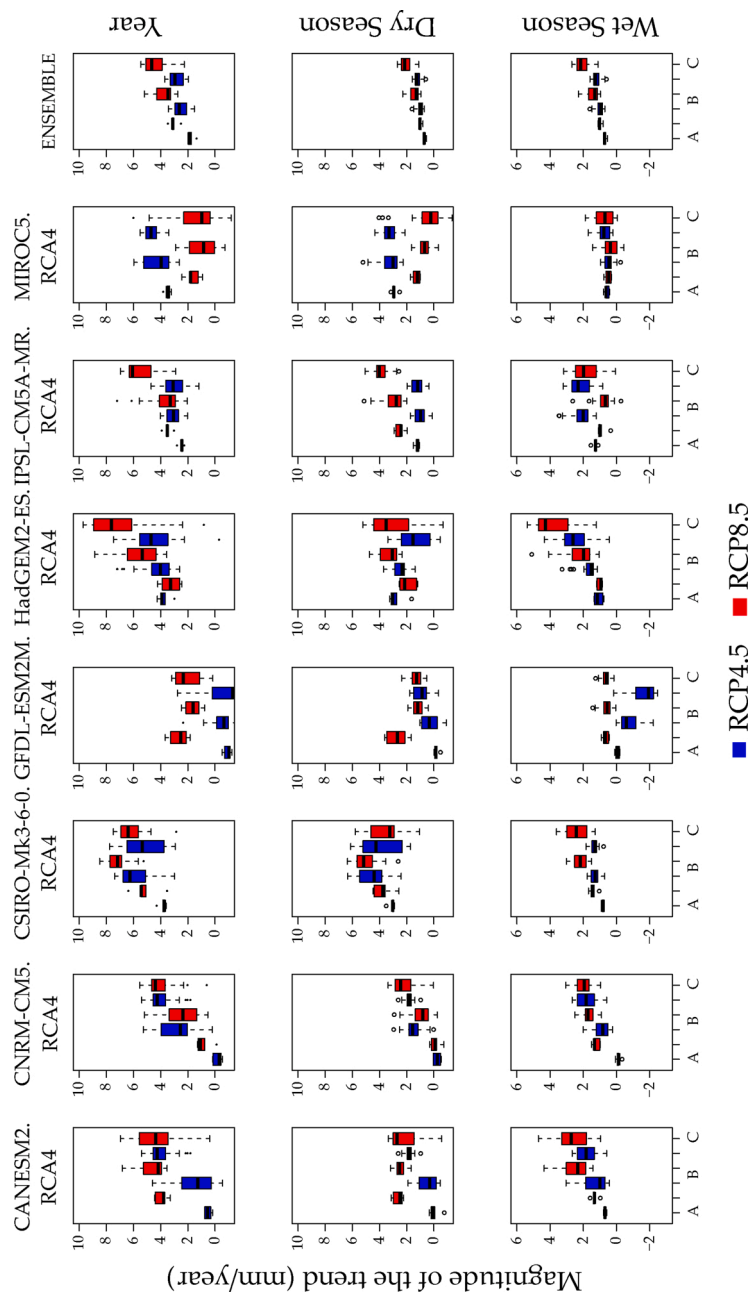

Fig. 11. Sen's slope of regional models at annual and seasonal scale over the period 2036-2065 (A: Guinean zone, B: Sudanian zone, C: Sahelian zone).

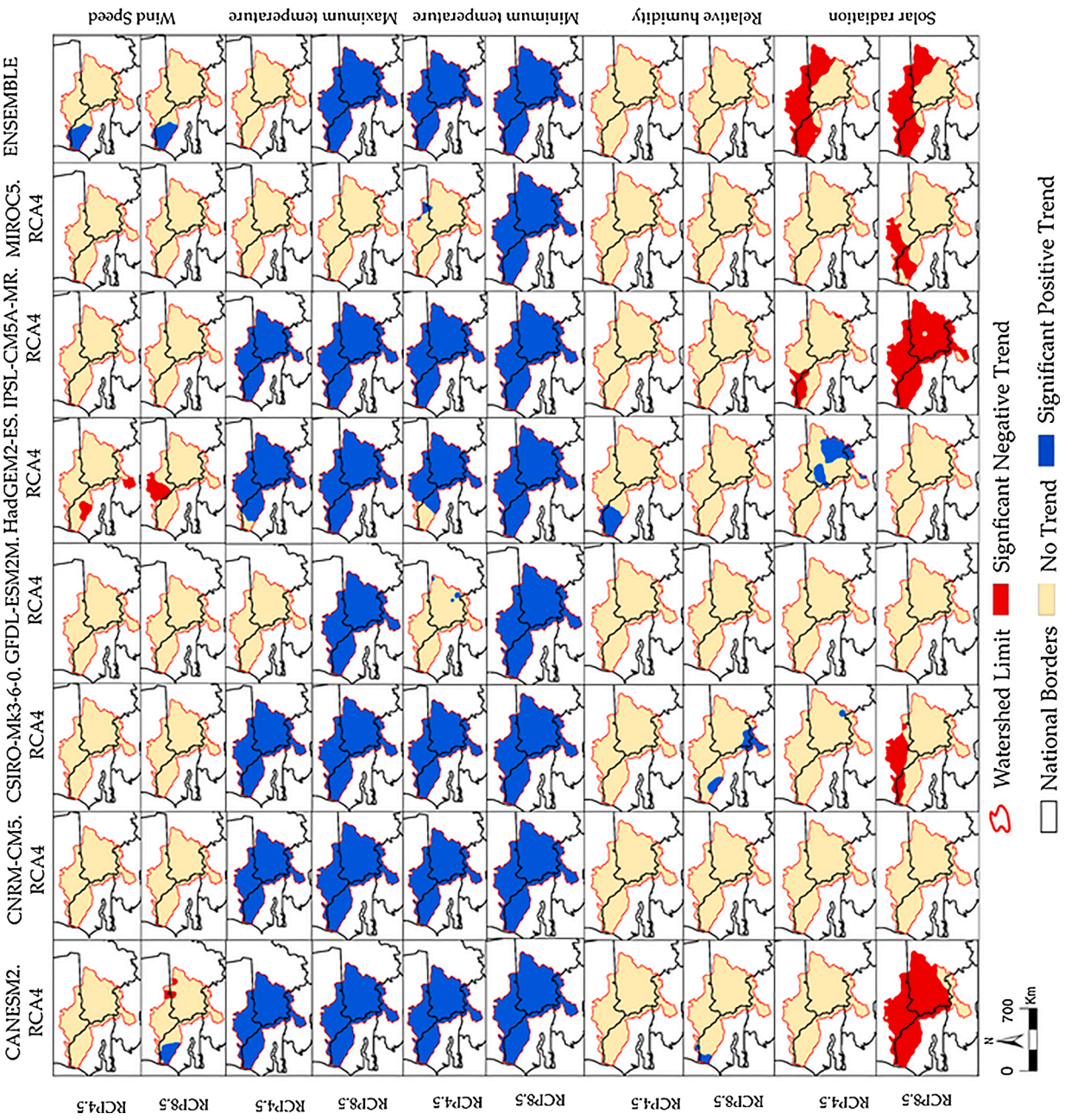
CANESM2. RCA4
CNRM-CM5. RCA4
CSIRO-Mk3-6-0. RCA4
GFDL-ESM2M. RCA4
HadGEM2-ES. RCA4
IPSL-CM5A-MR. RCA4
MIROC5. RCA4
ENSEMBLE
Solar radiation
Relative humidity
Minimum temperature
Maximum temperature
Wind Speed
RCP8.5
RCP4.5
RCP8.5
RCP4.5
RCP8.5
RCP4.5
RCP8.5
RCP4.5
RCP8.5
RCP4.5
Watershed Limit
National Borders
Signficant Negative Trend
No Trend
Significant Positive Trend
N
0
700
Km

Fig. 12. Spatial distribution of Mann Kendall's Z of the climate variables of regional models at annual scale over the period 2036 – 2065.

by 2065. According to the two scenarios, the annual average ET_0 increases respectively by 2.55 mm/year to 3.78 mm/year in the Sudanian zone and from 2.83 mm/year to 4.4 mm/year in the Sahelian zone.

The trend analysis shows that overall evapotranspiration will increase significantly ($p < 0.05$) by 2065 in the Senegal River Basin. Similar results are obtained by some studies across the world. Indeed, the work of Dong et al. (2019) pointed out a continuous increase in evapotranspiration throughout the 21 st century in China's semi-arid climate. Ndiaye et al. (2020b) showed a significant increase in the annual ET_0 in 32 % of the Senegal river basin during the period 1984−2017. However, Ndiaye et al. (2020b) also showed a significant drop in ET_0 in Sahelian area of the basin despite the increase in temperature. Here, projections do not reveal a drop in ET_0 and results indicate that this evaporation paradox will disappear from the basin by 2050. The increase in ET_0 could have impacts on the hydrological cycle and on agriculture. Indeed, from a hydrological point of view, the continuous increase in ET_0 can affect the rainfall effective and exacerbate the arid conditions of a given environment (Goyal, 2004). In agriculture sector, increasing ET_0 tends to increase aridity, decrease soil moisture and effective rainfall (Aubé, 2016). This increase in ET_0 could also lead to an increase in crop water demand and an increase in irrigation costs (Rahman et al., 2018).

3.5.2. *Future trends in climate variables*

Fig. 12 shows the future spatial distribution of Mann Kendall's Z of climate variables at the annual scale. All models agree on a significant increase in minimum and maximum temperatures with the exception of the RCP4.5 scenario of the NOAA-GFDL-ESM2M. RCA4 and MIROC5.RCA4 models which shows a non-significant trend in these two climate variables. A non-significant decrease ($p > 0.05$) in relative humidity was also noted over the entire basin.

Of all the models, only CANESM2.RCA4, HadGEM2-ES.RCA4, MIROC5.RCA4 and multi-model exhibit a significant decrease in wind speed and solar radiation. HadGEM2-ES.RCA4 showed a decrease in wind speed in 8% of the basin area for the RCP4.5 scenario and in 12 % of this for RCP8.5. This decrease in wind speed mentioned in Ndiaye et al. (2020b) is confirmed in future projections. In addition to the decrease in wind speed, some models show a significant decrease in solar radiation. Indeed, the ENSEMBLE shows a significant decrease in solar radiation for 46 % of the basin area according to the two scenarios. A significant decrease in radiation is also highlighted by IPSL-CM5A-MR.RCA4 in 11 % and 99 % of the basin according to the RCP4.5 and RCP8.5 scenarios, respectively. According to the RCP8.5 scenario, MIROC5.RCA4 and CANESM2.RCA4 respectively show a significant decrease in radiation in 21 % and 83 % of the basin area.

Table 4 gives a summary of Sen 'slope values of climate variables over the period 2036–2065 according to climatic zones. Considering the average of all the models, the minimum temperature varies from 0.02 °C/ year to 0.04 °C/year according to the RCP4.5 and RCP8.5 scenarios. The maximum temperature increases from 0.05 °C/year to 0.06 °C/year for RCP4.5 and from 0.01 °C/ year to 0.02 °C/year for RCP8.5. For maximum temperature, the low values obtained by ENSEMBLE RCP8.5 can be explained by the low values of CSIRO-Mk3−6-0.RCA4, HadGEM2-ES.RCA4 and MIROC5.RCA4. This indicates that the multi-model ensemble is not

Table 4
Summary of Sen's slope values (β per year) of climate variables at the annual scale (CA : CANESM2.RCA4, CN : CNRM-CM5.RCA4, SIR : CSIRO-Mk3-6-0.RCA4, GD : GFDL-ESM2M.RCA4, IP : IPSL-CM5A-MR.RCA4, MI : MIROC5.RCA4, MO : HadGEM2-ES.RCA4, ENS : ENSEMBLE).

Climate zones	Modèles	β(Minimum temperature)		β (Maximum temperature)		β (Wind speed)		β(Relative humidity)		β(Solar radiation)	
		RCP4.5	RCP8.5	RCP4.5	RCP8.5	RCP4.5	RCP8.5	RCP4.5	RCP8.5	RCP4.5	RCP8.5
Sudanian	CA	0.029	0.088	0.030	0.074	**−0.001**	**−0.001**	**−0.008**	**−0.014**	**−0.004**	**−0.007**
	CN	0.006	0.029	0.039	0.058	0.001	1.026	4.261	3.397	1.259	0.568
	CS	0.010	0.043	0.072	**−0.042**	0.002	1.251	3.971	5.117	**−0.730**	0.779
	GD	0.015	0.037	0.008	0.033	**−0.002**	**−0.001**	0.030	0.049	**−0.008**	**−0.001**
	MO	0.013	0.042	0.072	**−0.061**	0.002	1.850	5.150	5.080	**−1.093**	0.734
	IP	0.040	0.077	0.037	0.066	0.001	**−0.001**	**−0.050**	0.022	**−0.004**	**−0.010**
	MI	**−0.005**	0.015	0.056	**−0.052**	0.003	**−0.743**	1.199	3.531	**−1.040**	0.754
	ENS	0.004	0.031	0.060	0.001	**−0.025**	3.911	**−0.553**	6.864	0.625	**−0.731**
Guinean	CA	0.030	0.084	0.027	0.070	**−0.001**	0.000	**−0.019**	0.002	**−0.002**	0.001
	CN	**−0.001**	0.026	0.035	0.101	**−0.001**	**−0.029**	4.057	3.829	1.542	**−0.478**
	CS	0.018	0.035	0.074	**−0.001**	0.003	1.342	4.610	5.370	0.068	1.735
	GD	0.015	0.042	0.014	0.035	**−0.003**	0.001	0.047	0.008	0.000	0.003
	MO	0.025	0.032	0.062	**−0.015**	0.006	1.891	5.789	5.142	**−0.285**	**−0.750**
	IP	0.034	0.074	0.034	0.065	0.001	0.001	**−0.009**	0.005	0.002	**−0.011**
	MI	0.004	0.012	0.063	**−0.071**	0.001	0.332	1.131	3.854	**−1.656**	0.532
	ENS	0.002	0.025	0.058	0.000	**−0.001**	4.118	**−0.178**	6.994	0.634	0.612
Sahelian	CA	0.027	0.078	0.029	0.063	0.001	0.000	1.844	5.127	**−0.003**	**−0.007**
	CN	0.003	0.029	0.040	0.004	0.001	0.877	3.866	3.259	0.108	0.466
	CS	0.001	0.049	0.063	0.022	0.003	0.197	3.911	4.648	0.294	0.810
	GD	0.012	0.043	0.008	0.039	**−0.001**	**−0.002**	0.050	0.036	**−0.008**	**−0.003**
	MO	0.004	0.034	0.066	**−0.019**	0.000	0.675	3.257	4.891	**−0.484**	1.989
	IP	0.035	0.076	0.031	0.068	0.001	0.001	**−0.019**	0.012	**−0.004**	**−0.009**
	MI	**−0.004**	0.017	0.051	**−0.035**	0.002	**−0.655**	1.166	3.452	**−0.710**	0.659
	ENS	0.005	0.030	0.056	0.002	**−0.025**	3.627	**−0.862**	6.420	1.759	**−1.603**

always preferable as it here leads to a lower, incongruous increase in temperature with RCP8.5 than with RCP4.5. Moreover, for the RCP4.5, the models show that the maximum temperature will increase from 1.3 to 2.5 °C in Guinean zone, 1.3–2.7 °C in Sudanian zone and from 1.3 to 2.8 °C in Sahelian one. For the RCP8.5 the high values of maximum temperature vary between 3.1 and 3.3 °C depending on climate zones. The minimum temperature will respectively increase by 2.9, 3.2 and 3.3 °C in Guinean, Sudanian and Sahelian zones under RCP4.5. According to RCP8.5, the minimum temperature will vary between 3.2–3.9 °C according to the climate models. The maximum values are noted in Sahelian and Sudanian zones. It is also important to note that the minimum temperatures increase faster than the maximum ones. The same results are obtained by Ly et al. (2013) in West Africa and Samba and Nganga (2014) in Congo Brazzaville who noted that the increase of minimum temperature is more important than the maximum. This situation may be explained by the concentration of aerosol which reduce the solar radiation reaching the earth surface (Ringard et al., 2014). This increase in temperature can also affect crops. For example, Diop (2009) mentioned that ecological monitoring carried out in Nianga (Podor, Senegal River Basin) showed that certain varieties of rice have abortion rates of 33–57% when the temperature exceeds 35 °C.

Relative humidity varies from 0.17 to 7%/year in the Guinean zone, from -0.6–7% in the Sudanese one and from -0.9 to 6%/year in the Sahelian zone according to the two scenarios. Wind speed and solar radiation vary respectively from -0.025 to 4.11 m/year and from -1.6 to 1.7 $MJ.m^{-2}{}_{D}{}^{-1}$/year depending on both scenarios and depending on climatic zones. On a seasonal scale, all models predict a significant increase in temperatures during the dry and rainy season. The models also predict an insignificant decrease in wind speed and relative humidity during both seasons. The downward trend in solar radiation is generally insignificant on a seasonal scale.

Trend analysis show a significant increase in temperatures in the Senegal River basin. This rise in temperatures would be considered the main reason for the significant increase in evapotranspiration in the period 2036–2065. This information associated with the trend of ET_0 and climate variable allow to note that horizon 2036–2065 will not be stationary and the climate will continue to change if the temperature increase at the current rate. Indeed, significant positive trend is both ET_0 and temperatures, is showed by RCMs. This confirms the studies by Abiye et al. (2019) and Ndiaye et al. (2020b) according to which the temperature (maximum and minimum) is the main factor of variation of evapotranspiration during the periods 1906–2015 and 1984–2017 in West Africa and in the Senegal river basin. Of all the variables, only wind speed and solar radiation show a significant decrease depending on the models. The decrease in wind speed (Wind Stilling) and solar radiation (Global Dimming) explains the decrease in evapotranspiration mentioned by some authors (McVicar et al., 2012; Chu et al., 2017; Han et al., 2019; Bian et al., 2020; Ndiaye et al., 2020b). This decrease in solar radiation is linked to the concentration of aerosols in the atmosphere due to human activities (Han et al., 2019).

4. Conclusion

The results of this study show that the ET_0 values obtained by the RCMs are closer to those of the reanalyses than the GCMs, though they tend to overestimate ET_0. Trend analysis shows almost all models agree on a significant increase in reference evapotranspiration in the period 2036–2065 under the RCP4.5 and RCP8.5 scenarios. The ENSEMBLE provides an increase in ET_0 of 39 mm for RCP4.5 and 144 mm for RCP8.5 in the Guinean zone. In the Sudanese and Sahelian zones, ET_0 will increase respectively from 48 mm to 266 mm and from 57 mm to 277 mm according to the two scenarios. Trends in climate variables show a significant increase in maximum and minimum temperatures. This rise in temperatures is shown to be the primary explanation for the increase in ET_0 though some models also highlight a significant decrease in wind speed and solar radiation. Sensitivity analysis reveals that ET_0 is more sensitive to relative humidity, maximum temperature and solar radiation. The increase in the future will increase crop water requirements, accentuate water losses in reservoirs, reduce hydroelectric deliverability and increase competition between different users. It is important to note that this increase of ET_0 will not be stationary in 2065 and may continue to increase if the temperatures rise at the same rate. Furthermore, this work underlines the discrepancies between results based on GCMs and RCMs as well as those between individual RCMs when estimating evapotranspiration. These differences highlight the importance of improving the performance of climate circulation models (both GCMs and RCMs) to allow for a more accurate and reliable estimate of climate variables needed to analyze long-term ET_0 variations/projections. It would also be important to have complete in-situ meteorological observations to fill in the gaps and improve climate simulations.

Author statement

Conceptualization, P.M.N, A.B. and L.D.; methodology, P.M.N, A.B. and L.D.; software, P.M.N, A.B. and L.D.; validation, A.B., L.D., A.D (Alain Dezetter), E.G., A.D (Abdoulaye Deme)., A.O; formal analysis, A.B., L.D., A.D (Alain Dezetter), E.G., A.D (Abdoulaye Deme)., A.O; investigation, P.M.N, A.B., L.D, A.D (Alain Dezetter)., E.G; data curation, P.M.N; writing—original draft preparation, P.M.N, A.B. and L.D.; writing—review and editing, P.M.N, A.B., L.D., A.D (Alain Dezetter), E.G., A.D (Abdoulaye Deme)., A.O; visualization, P.M.N, A.B. and L.D.; supervision, A.B., L.D., A.D (Alain Dezetter), E.G., A.D (Abdoulaye Deme)., A.O; project administration, A.B; funding acquisition, A.O, A.B. All authors have read and agreed to the published version of the manuscript.

Funding

This research was partially funded by the AICS/UE N. 03/2020/WEFE-SENEGAL project.

Declaration of Competing Interest

The authors declare that there is no conflict of interests regarding publishing this article.

Acknowledgments

Reanalysis weather data used in this study were obtained from the NASA Langley Research Center (LaRC) POWER Project funded through the NASA Earth Science. The authors also wish to thank the two anonymous reviewers and the special academic editor for their suggestions, which helped improve the manuscript.

Appendix A. Supplementary data

Supplementary material related to this article can be found, in the online version, at doi:https://doi.org/10.1016/j.ejrh.2021.100820.

References

Abiye, O.E., Matthew, O.J., Sunmonu, L.A., Babatunde, O.A., 2019. Potential Evapotranspiration Trends in West Africa From 1906 to 2015. Springer Nature, Switzerland, pp. 1–14. https://doi.org/10.1007/s42452-019-1456-6.

Allen, R., Pereira, L., Raes, D., Smith, M., 1998. Crop Evapotranspiration. Guideline for Computing Crop Requirements. FAO-Irrigation and drainage paper 56, Rome.

Aubé, D., 2016. Impacts Du Changement Climatique Dans Le Domaine De l'eau Sur Les Bassins Rhône-méditerranée Et Corse - Bilan Actualisé Des Connaissances. Collection « Eau & Connaissance ». Agence de l'eau Rhône Méditerranée Corse, p. 114 pages.

Bahir, M., Ouhamdouch, S., Ouazar, D., El Moçayd, N., 2020. Climate change effect on groundwater characteristics within semi-arid zones from western Morocco. Groundw. Sustain. Dev. 11, 1–14. https://doi.org/10.1016/j.gsd.2020.100380.

Bian, Y., Dai, H., Zhang, Q., Yang, L., Du, W., 2020. Spatial distribution of potential evapotranspiration trends in the Inner Mongolia autonomous Region (1971–2016). Theor. Appl. Climatol. https://doi.org/10.1007/s00704-020-03154-y.

Bodian, A., Dezetter, A., Diop, L., Deme, A., Djaman, K., Diop, A., 2018. Future climate change impacts on streamflows of Two Main West Africa river basins: senegal and Gambia. Hydrology 5, 21. https://doi.org/10.3390/hydrology5010021.

Bodian, A., Diop, L., Panthou, G., Dacosta, H., Deme, A., Dezetter, A., Ndiaye, P.M., Diouf, I., Vichel, T., 2020. Recent trend in hydroclimatic conditions in the Senegal River Basin. Water 12, 436. https://doi.org/10.3390/w12020436.

Chaouche, K., Neppel, L., Dieulin, C., Pujol, N., Ladouche, B., Martin, E., Salas, D., Caballero, Y., 2010. Analyses of precipitation, temperature and evapotranspiration in a French Mediterranean region in the context of climate change. IEEE Trans. Geosci. Remote Sens. 342, 234–243.

Chu, R., Li, M., Shen, S., Islam, A., Cao, W., Tao, S., Gao, P., 2017. Changes in reference evapotranspiration and its contributing factors in Jiangsu, a major economic and agricultural province of Eastern China. Water 9, 486. https://doi.org/10.3390/w9070486.

Delghandi, M., Joorabloo, S., Emamgholizadeh, S., 2017. Climate change impacts on spatial-temporal variations of reference evapotranspiration in Iran. Water Harvesting Res. 2 (1), 13–23. https://doi.org/10.22077/jwhr.2017.592.

Dione, O., 1996. Evolution Climatique Récente Et Dynamique Fluviale Dans Les Hauts Bassins Des Fleuves Sénégal Et Gambie (Recent Climate Evolution and Fluvial Dynamics in the High Basins of the Senegal and Gambia Rivers). Ph.D. Thesis. Université de Lyon 3 Jean Moulin, ORSTOM, Paris, France, p. 438p (In French). Available online: http://horizon.documentation.ird.fr/exldoc/pleins_textes/pleins_textes_7/TDM_7/010012551.pdf (accessed on 10 March 2020).

Diop, M., 2009. Les Bilans Hydriques Dans La Moyenne Vallée Du Fleuve Sénégal-contribution à l'étude Des Besoins En Eau, Thèse De Doctorat En Géographie. Université de Paris 1, Paris, p. 375p.

Dong, Q., Wang, W., Shao, Q., Xing, W., Ding, Y., Fu, J., 2019. The response of reference evapotranspiration to climate change in Xinjiang, China: historical changes, driving forces, and future projections. Int. J. Climatol. 40, 235–254. https://doi.org/10.1002/joc.6206.

Giménez, P.O., García-Galiano, S.G., 2018. Assessing regional climate models (RCMs) ensemble-driven reference evapotranspiration over Spain. Water 10, 1181. https://doi.org/10.3390/w10091181.

Goyal, R.K., 2004. Sensitivity of evapotranspiration to global warming:a case study of arid zone of Rajasthan (India). Agric. Water Manag. 69, 1–11. https://doi.org/10.1016/j.agwat.2004.03.014.

Gupta, H.V., Kling, H., Yilmaz, K.K., Martinez, G.F., 2009. Decomposition of the mean squared error and NSE performance criteria: implications for improving hydrological modeling. J. Hydrol. 377, 80–91.

Han, J., Zhao, Y., Wang, J., Zhang, B., Zhu, Y., Jiang, Sh., Wang, L., 2019. Effects of different land use types on potential evapotranspiration in the Beijing-Tianjin Hebei region, North China. J. Geogr. Sci. 29 (6), 922–934. https://doi.org/10.1007/s11442-019-1637-7.

Huo, Z., Dai, X., Feng, S., Kang, S., Huang, G., 2013. Effect of climate change on reference evapotranspiration and aridity index in arid region of China. J. Hydrol. 492, 24–34. https://doi.org/10.1016/j.jhydrol.2013.04.011.

IPCC, 2014. In: the Core Editorial Team, Pachauri, R.K., Meyer, L.A. (Eds.), Climate Change 2014: Synthesis Report. Contribution of Working Groups I, II and III to the Fifth Assessment Report of the Intergovernmental Panel on Climate Change. IPCC, Geneva, Switzerland, p. 161 p.

IPCC, 2018. In: Masson-Delmotte, V., Zhai, P., Pörtner, H.O., Roberts, D., Skea, J., Shukla, P.R., Pirani, A., Moufouma-Okia, W., Péan, C., Pidcock, R., Connors, S., Matthews, J.B.R., Chen, Y., Zhou, X., Gomis, M.I., Lonnoy, E., Maycock, T., Tignor, M., Waterfield, T. (Eds.), Summary for Policymakers, Global Warming 1.5 ° C, IPCC Special Report on the Consequences of Global Warming 1.5 °C Relative to Pre-Industrial Levels and Associated Pathways of Global Gas Emissions Greenhouse Effect, in the Context of Strengthening the Global Response to Climate Change, Sustainable Development and the Fight Against Poverty. World Meteorological Organization, Geneva, Switzerland, p. 32 p.

Kendall, M.G., 1975. Rank Correlation Methods. Hafner, New York.

Li, Y., Feng, A., Liu, W., Ma, X., Dong, G., 2017. Variation of aridity index and the role of climate variables in the Southwest China. Water 2017 (9), 743. https://doi.org/10.3390/w9100743.

Lin, P., He, Z., Du, J., Chen, L., Zhu, X., Li, J., 2018. Impacts of climate change on reference evapotranspiration in the Qilian Mountains of China: historical trends and projected changes. Int. J. Climatol. https://doi.org/10.1002/joc.5477.

Ly, M., Traoré, S.B., Alhassane, A., Sarr, B., 2013. Evolution of some observed climate extremes in the West African Sahel ». Weather Clim. Extrem. 1, 19–25.

Malamos, N., Tsirogiannis, I.L., Tegos, A., Efstratiadis, A., Koutsoyiannis, D., 2017. Spatial interpolation of potential evapotranspiration for precision irrigation purposes. Eur. Water 59, 303–309.

Mann, H.B., 1945. Non-parametric test against trend. Econometrika 13, 245e259.

Martins, D.S., Paredes, P., Raziei, T., Pires, C., Cadimad, J., Pereira, L.S., 2016. Assessing reference evapotranspiration estimation from reanalysis weather products. An application to the Iberian Peninsula. Int. J. Climatol. 1–20. https://doi.org/10.1002/joc.4852.

McVicar, T.R., Roderick, M.L., Donohue, R.J., Li, T.L., Niel, T.G.V., Thomas, A., Grieser, J., Jhajharia, D., Himri, Y., Mahowald, N.M., 2012. Global review and synthesis of trends in observed terrestrial near-surface wind speeds: implications for evaporation. J. Hydrol. 416–417, 182–205.

Moratiel, R., Snyder, R.L., Durán, J.M., Tarquis, A.M., 2011. Trends in climatic variables and future reference evapotranspiration in Duero Valley (Spain). Nat. Hazards Earth Syst. Sci. 11, 1795–1805. https://doi.org/10.5194/nhess-11-1795-2011.

Mubialiwo, A., Onyutha, C., Abebe, A., 2020. Historical rainfall and evapotranspiration changes over mpologoma catchment in Uganda, hindawi. Adv. Meteorol. 19 pages. https://doi.org/10.1155/2020/8870935.

Ndiaye, P.M., Bodian, A., Diop, L., Deme, A., Dezetter, A., Djaman, K., 2020a. Evaluation and calibration of alternative methods for estimating reference evapotranspiration in the Senegal River Basin. Hydrology 7, 24. https://doi.org/10.3390/hydrology7020024.

Ndiaye, P.M., Bodian, A., Diop, L., Deme, A., Dezetter, A., Djaman, K., Ogilvie, A., 2020b. Trend and Sensitivity Analysis of Reference Evapotranspiration in the Senegal River Basin Using NASA Meteorological Data. Water 12, 1957. https://doi.org/10.3390/w12071957.

Obada, E., Alamou, E.A., Chabi, A., Zandagba, J., Afouda, A., 2017. Trends and changes in recent and future penman-monteith potential evapotranspiration in Benin (West Africa). Hydrology 4 (38), 1–19. https://doi.org/10.3390/hydrology4030038.

Ouhamdouch, S., Bahir, M., Ouazar, D., Goumih, A., Zouari, K., 2020. Assessment the climate change impact on the future evapotranspiration and flows from a semi-arid environment. Arab. J. Geosci. https://doi.org/10.1007/s12517-020-5065-x.

Poccard-Leclercq, I., 2000. Etude Diagnostique De Nouvelles Données Climatiques : Les Réanalyses. Exemples d'application Aux Précipitations En Afrique Tropicale. Géographie. Ph.D. Thesis. Université de Bourgogne, Dijon, France, p. 255p. Available online : https://tel.archives-ouvertes.fr/tel-00012042/document (accessed on 8 March 2020).

Qi, P., Zhang, G., Xu, Y.J., Wu, Y., Gao, Z., 2017. Spatiotemporal changes of reference evapotranspiration in the highest-latitude region of China. Water 9, 493.

Rahman, M.A., Yunsheng, L., Sultana, N., Ongoma, V., 2018. Analysis of reference evapotranspiration (ET0) trends under climate change in Bangladesh using observed and CMIP5 data sets. Meteorol. Atmos. Phys. https://doi.org/10.1007/s00703-018-0596-3.

Ringard, J., Dieppois, B., Rome, S., Dje, K.B., Konaté, D., Katiellou, G.L., Lazoumar, R.H., Bouzou-Moussa, I., Konaré, A., Diawara, A., Ochou, A.D., Assamoi, P., Camara, M., Diongue, A., Descroix, L., Diedhiou, A., 2014. Évolution des pics de températures en Afrique de l'ouest : étude comparative entre Abidjan et Niamey », 27. 27e Colloque de l'Association International de Climatologie, "Système et Interactions", Dijon, France, pp. 1–7.

Samba, G., Nganga, D., 2014. Minimum and maximum temperature trends in Congo-Brazzaville: 1932-2010 ». Atmos. Clim. Sci. 4, 404–430.

Sarkar, S., Sarkar, S., 2018. A review on impact of climate change on evapotranspiration. Pharma Innovation J. 7 (11), 387–390.

SDAGE-OMVS, 2009. Etat Des Lieux Et Diagnostique ; Rapport Provisoire 2009, Rapport De Phase III. SDAGE-OMVS, Dakar, Senegal, p. 2011.

Tao, X., Chen, H., Xu, Ch., Hou, Y.-K., Jie, M., 2015. Analysis and prediction of reference evapotranspiration with climate change in Xiangjiang River Basin, China. Water Sci. Eng. 8 (4), 273 e 281.

Taylor, K.E., Stouffer, R.J., Meehl, G.A., 2012. An overview of CMIP5 and the experiment design. Bull. Am. Meteorol. Soc. 93, 485–498.

Wang, Z., Ye, A., Wang, L., Liu, K., Cheng, L., 2019. Spatial and temporal characteristics of reference evapotranspiration and its climatic driving factors over China from 1979–2015. Agri. Water Manage. (213), 1096–1108. https://doi.org/10.1016/j.agwat.2018.12.006.

Wilcox, C., Vischel, T., Panthou, G., Bodian, A., Blanchet, J., Descroix, L., Quantin, G., Cassé, C., Tanimoun, B., Kone, S., 2018. Trends in hydrological extremes in the Senegal and niger rivers. J. Hydrol. 566 (2018), 531–545. https://doi.org/10.1016/j.jhydrol.2018.07.063.

Yang, L., Feng, Q., Adamowski, J.F., Yin, Z., Wen, X., Wu, M., Jia, B., Hao, Q., 2020. Spatio-temporal Variation of Reference Evapotranspiration in Northwest China Based on CORDEX-EA. https://doi.org/10.1016/j.atmosres.2020.104868.

Yin, Yunhe, Ma, Danyang, Wu, Shaohong, Pan, Tao, 2015. Projections of aridity and its regional variability over China in the mid-21st century. Int. J. Climatol. 35 (14), 4387–4398. https://doi.org/10.1002/joc.4295.

Zhao, L., Xia, J., Sobkowiak, L., Li, Z., 2014. Climatic characteristics of reference evapotranspiration in the Hai River Basin and their attribution. Water 6, 1482–1499. https://doi.org/10.3390/w6061482.